

TOPICAL REVIEW • OPEN ACCESS

## Real space analysis of colloidal gels: triumphs, challenges and future directions

To cite this article: C Patrick Royall *et al* 2021 *J. Phys.: Condens. Matter* **33** 453002

View the [article online](#) for updates and enhancements.



**IOP | ebooks™**

Bringing together innovative digital publishing with leading authors from the global scientific community.

Start exploring the collection—download the first chapter of every title for free.

## Topical Review

# Real space analysis of colloidal gels: triumphs, challenges and future directions

C Patrick Royall<sup>1,2,3,4,\*</sup> , Malcolm A Faers<sup>5</sup>, Sian L Fussell<sup>3,6</sup>  and James E Hallett<sup>7</sup> 

<sup>1</sup> Gulliver UMR CNRS 7083, ESPCI Paris, Université PSL, 75005 Paris, France

<sup>2</sup> HH Wills Physics Laboratory, Tyndall Avenue, Bristol, BS8 1TL, United Kingdom

<sup>3</sup> School of Chemistry, University of Bristol, Cantock Close, Bristol, BS8 1TS, United Kingdom

<sup>4</sup> Centre for Nanoscience and Quantum Information, Tyndall Avenue, Bristol, BS8 1FD, United Kingdom

<sup>5</sup> Bayer AG, Crop Science Division, Formulation Technology, Alfred Nobel Str. 50, 40789 Monheim, Germany

<sup>6</sup> Bristol Centre for Functional Nanomaterials, University of Bristol, Tyndall Avenue, Bristol, BS8 1TL, United Kingdom

<sup>7</sup> Physical and Theoretical Chemistry Laboratory, South Parks Road, University of Oxford, OX1 3QZ, United Kingdom

E-mail: [paddy.royall@espci.fr](mailto:paddy.royall@espci.fr)

Received 7 January 2021, revised 6 April 2021

Accepted for publication 25 May 2021

Published 31 August 2021



## Abstract

Colloidal gels constitute an important class of materials found in many contexts and with a wide range of applications. Yet as matter far from equilibrium, gels exhibit a variety of time-dependent behaviours, which can be perplexing, such as an increase in strength prior to catastrophic failure. Remarkably, such complex phenomena are faithfully captured by an extremely simple model—‘sticky spheres’. Here we review progress in our understanding of colloidal gels made through the use of real space analysis and particle resolved studies. We consider the challenges of obtaining a suitable experimental system where the refractive index and density of the colloidal particles is matched to that of the solvent. We review work to obtain a particle-level mechanism for rigidity in gels and the evolution of our understanding of time-dependent behaviour, from early-time aggregation to ageing, before considering the response of colloidal gels to deformation and then move on to more complex systems of anisotropic particles and mixtures. Finally we note some more exotic materials with similar properties.

Keywords: gels, colloidal gels, spinodal decomposition

(Some figures may appear in colour only in the online journal)

\* Author to whom any correspondence should be addressed.

 Original content from this work may be used under the terms of the [Creative Commons Attribution 4.0 licence](#). Any further distribution of this work must maintain attribution to the author(s) and the title of the work, journal citation and DOI.

## 1. Background and motivation

The formation of a network of arrested material with high but finite zero-shear viscosity upon slight quenching is among the most striking features of condensed matter [1–5]. Such gels are absolutely the stuff of everyday life, for example gels comprise our tissues, numerous foods, cosmetics, coatings, crop protection suspension formulations, pharmaceutical suspension formulations, pigment printing inks, dispersions for 3D printing, ceramic preparations, food preparations, detergent formulations and numerous home care products [6–9]. A wide range of materials also exhibit gelation including proteins [10–14], granular matter [15, 16], phase-demixing oxides [17], and metallic glassformers [18]. Indeed so wide is the range of materials that are commonly termed gels—from polymer gels, hydrogels, and colloidal gels—that these materials in fact obey very different physics. Some materials, notably polymers and some colloidal systems [19], can undergo *equilibrium* gelation, and from a thermodynamic perspective can be regarded as being rather similar to supercooled liquids [20]. Some of these systems form a network stabilised by their disinclination to condense, effectively being an *empty liquid* [21].

Unlike equilibrium gels, many (but not all [19, 20, 22]) colloidal gels form via the process of *arrested phase separation*. The system begins to phase separate, typically in a spinodal-like fashion [23] and often with a bicontinuous texture (figures 1 and 2). After demixing is initiated, what then happens is that one (or, in principle, both) demixing phases undergo dynamical arrest which results in a solid-like material, a gel. This is an example of *viscoelastic phase separation*, which pertains to the case where the demixed phases have significantly different viscosities [1]. These gels then represent an example of *matter far from equilibrium* as the thermodynamic equilibrium would be phase separated colloid-rich and colloid-poor states [2]. The colloid-rich phase can exist as colloidal crystals for colloids of low polydispersity in shallow quenches [2, 24] and amorphous networks for deeper quenches [25–27]. This has two interesting consequences: first the properties of the network are not constant but age over time, and second they depend on the shear and processing history, which is of particular importance for formulated products and their manufacturing process.

To obtain such ‘spinodal’ gels, a few systems are suitable candidates. Typically (though not always [28]), an attraction between the colloidal particles is present. Such an attraction may result from van der Waals attractions [29, 30], or from polymer-induced depletion [2, 24, 31, 32], bridging by telechelic (triblock) copolymers [33–35] or critical Casimir interactions [36–40]. Some evidence has been found for gelation-like behaviour, in the form of a percolating network, in *active colloidal systems* with microtubules [41] and colloids with dipolar interactions [42]. Of these, the most common and most well-studied in real space, are depletion gels of spherical colloids and non-absorbing polymer, and these form our primary focus [2]. Indeed so dominant are studies of ‘spinodal gels’ and even of one particular system (see section 4.1) that we may argue in favour of studying a wider

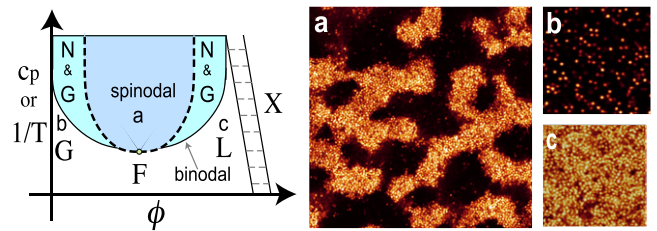


**Figure 1.** Schematic of colloid–polymer mixture phase diagram in the case that the effective interaction is *long-ranged*, polymer colloid size ratio  $q > 0.3$ . Here G is a (colloidal) gas, L a liquid, X a crystal and F a (supercritical) fluid. The binodal line marks the limit of the gas–liquid phase coexistence (shaded region). Nucleation and growth is denoted as N & G, the spinodal line is the thick dashed line. (a) A colloidal system undergoing spinodal decomposition, state point is located in the main panel as ‘a’. (b) A colloidal gas, state point is located as ‘b’. (c) A colloidal liquid, state point is located as ‘c’.

range of systems with a view to exploring other gelation mechanisms for example. We consider work that has been carried out on other systems towards the end of the review in section 7. Often these also exhibit ‘spinodal gelation’, so the mechanism can be quite similar, even if the interactions have a different origin (such as critical Casimir interactions [39]).

Here, we consider what has been learnt about the nature of colloidal gelation using the technique of *real space analysis*, and in particular imaging of individual colloidal particles via confocal microscopy—*particle-resolved studies* [43]. We enquire as to the utility of this technique to address the challenges presented by colloidal gels. We note that a salient strength of the technique is its ability to investigate local phenomena, and thus to address the perceived wisdom of materials science that *the microscopic structure determines the dynamics and macroscopic behaviour of the material* [44].

*The case for ‘sticky spheres’.*—It is worth noting that if hard spheres may be taken as being surprisingly rich in their behaviour, given that the system is driven only by entropy, then, since the seminal work of Baxter [45] the addition of a short-range attraction, i.e. ‘sticky spheres’, opens up a plethora of new phenomena. These include (metastable) liquid–gas phase coexistence and accompanying criticality [46], in addition to gelation and a multitude of arrest mechanisms [2, 5, 47, 48]. We suggest that such sticky spheres may be taken as a minimal model for certain classes of matter far from equilibrium and emphasise that approximations to sticky spheres concern much of the material presented here.

### 1.1. Pressing challenges in colloidal gelation

We have seen from the discussion above that gels sit at the overlap between phase separation via spinodal decomposition (section 2.1) and the glass transition (section 2.2). If this is how colloidal gels come about, what can we say about their properties?

- As non-equilibrium systems, gels age.
- A consequence of ageing is that the properties of gels change over time, and one such property is an increase in mechanical strength.

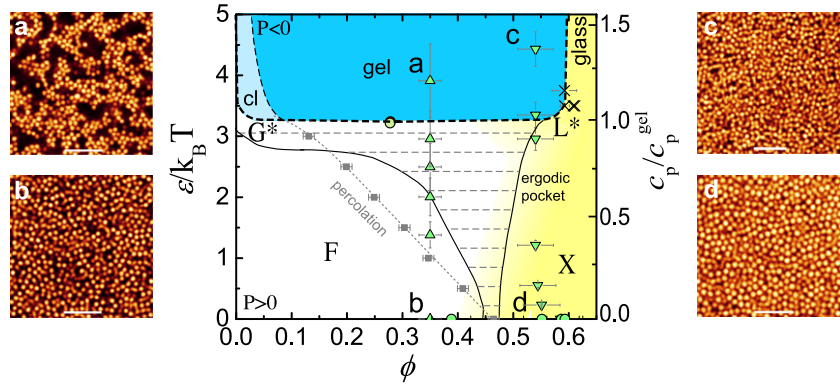


**Figure 2.** Phase diagram for spinodal decomposition for spheres with a short-ranged attraction (square well with range  $0.03\sigma$ ). Blue shaded region bounded by thick black dashed line denotes region of spinodal decomposition. Dynamical arrest due to vitrification is shown in shaded yellow regions. Pale shaded region (cl) pertains to cluster-growth driven gelation reflecting the fact that at low volume fraction, there are insufficient colloids to form a percolating network at short times. However the system is still thermodynamically unstable and undergoes spinodal decomposition (section 2.1). Here gelation is time-dependent with a percolating network emerging after some time [77, 80]. Experimental data for a colloid–polymer mixture with a short-ranged interaction,  $q \approx 0.18$  is mapped onto this phase diagram (green data points). State points (a)–(d) are located as shown in the phase diagram. Percolation is indicated by the grey line and is distinct from gelation. Bars = 20  $\mu\text{m}$ . Reprinted from [48], with the permission of AIP Publishing.

- Another consequence is their low reproducibility since the early stage network structure formed depends on its quenching history and mechanical processing history.
- Paradoxically, although they become stronger over time, gels often fail under their own weight, catastrophically, after a waiting time, which may extend to months or years, when little seems to happen.

Non-equilibrium arrested colloidal gels are ubiquitous among everyday formulated products and a key requirement is that they maintain their physical stability and performance during their service life, which can be up to several years. This is imparted by the mechanical strength of the arrested gel network and limited by its ageing rate (which is often temperature dependent), external mechanical disturbances (for example during transport and handling) and gravitational stresses experienced during storage. Notably, in the material response to these, the size and shape of the container plays a surprisingly important role. There is therefore an important need for improved knowledge on ageing of colloidal gels and a better ability to reliably predict their shelf life stability.

## 1.2. Scope and aims of this review

Gels constitute a wide and somewhat ill-defined range of materials. Here we consider *colloidal* gels, which themselves have been subjected to a very wide range of analysis, including theory [24, 49–54] and computer simulation [55–58]. Experimental techniques include rheology [59–61], direct observation and video imaging [62, 63] and scattering [2, 64–66]. This has led to great insight, and has been reviewed previously [3, 5]. However we focus here on real space analysis using 3D confocal microscopy with an emphasis on particle-resolved studies. To our knowledge, while particle resolved techniques for colloids have been reviewed [43] which briefly covers some early work on gels, no review focussing on gels exists, and that forms the purpose of this work. Where possible, we have referenced relevant review papers, but in any case humbly ask

for patience on the part of readers regarding those papers we have missed, or where our opinion seems at odds with theirs. We nevertheless hope to convey the exciting progress made by using real space analysis to study colloidal gels.

This review is organised as follows. Given the wide variety of materials which undergo colloidal gelation, and the broad interest from the basic physics of model far-from-equilibrium systems to a large number of applications, those working with colloidal gels come from a number of disciplines. We have therefore made some attempt to provide sufficient material to cover the underlying physics. Those familiar with spinodal decomposition and/or dynamical arrest may wish to skip the overviews in sections 2.1 and 2.2 respectively. In section 3 we detail mechanisms of attraction between colloids that lead to gelation. Similarly, readers familiar with these may wish to skip this section. In section 4.1 we review early work on real space analysis of colloidal gels and discuss the consequences of the unexpected degree of electrostatic charging present in the refractive index matched and density matched systems used. In section 4.2, we review key developments that provided compelling evidence for spinodal decomposition as the mechanism for colloidal gelation in the context of other proposed mechanisms. In section 4.3, we consider the use of real space analysis to provide local mechanisms for dynamical arrest in colloidal gels. Section 5 details the dynamical properties of colloidal gels, and these fall into the following categories. Short-time dynamics with little change in the overall properties are discussed in section 5.1, while changes in the nature of the gel are reviewed in section 5.2. Gravitational collapse is considered in section 5.3 and this leads us to emphasise connections between model systems and real world products in section 5.4. The response to deformation is considered in section 5.5. We then move on to consider the introduction of complexity in depletion systems in section 6 before discussing more exotic forms of (colloidal) gels in section 7. We conclude with an outlook in section 8.

## 2. The mechanism of gelation via arrested spinodal decomposition: matter far-from-equilibrium meets the glass transition

Understanding gelation—and the mechanism by which gels form invokes two grand challenges of modern physics: matter far from equilibrium and dynamical arrest. Firstly, at least in the context of gelation, the matter far-from-equilibrium aspect pertains to spinodal decomposition, which at a mean field level is reasonably well understood, beginning with the seminal work of Cahn and Hilliard [23, 67, 68].

The second, the glass transition was famously described as ‘the deepest problem in condensed matter physics’ by Philip Anderson in 1996 and since then great progress has been made, see e.g. [58, 69–71] for reviews and [72–75] for shorter perspectives. However it is fair to say that the problem of the glass transition may be regarded as being solved only for hyperspheres in high dimension (which is also mean field) [76].

### 2.1. Brief overview of spinodal decomposition

We now outline spinodal decomposition in the context of colloidal gelation. Figure 1 is a schematic of a phase diagram for a colloid–polymer mixture whose effective colloid–colloid interaction is long-ranged, the polymer–colloid size ratio is  $q > 0.3$ . For such a system, the colloidal liquid (L in figure 1) is thermodynamically stable (see section 3) [24]. At the binodal line in a colloid–polymer mixture, the chemical potential of the demixed colloidal gas–colloidal liquid system is the same as the one-phase fluid. However, for sufficient quenching (or, in the case of colloid–polymer mixtures, polymer concentration) the system is unstable even to small fluctuations in composition—*spinodal decomposition*—as shown by the dashed line in figure 1. Here we shall denote composition by  $c$  noting that for colloid–polymer mixtures this means the colloid volume fraction  $\phi_c$  and polymer concentration  $c_p$  which are coupled [24]. The canonical treatment is Cahn–Hilliard theory [67, 68].

We start with a Landau–Ginzburg free energy, which amounts to the observation that because any gradients in concentration  $c$  are vectors, and the free energy itself is a scalar, then the lowest-order term will be  $\mathcal{O}(\nabla c)^2$ . The free energy of the system of volume  $V$  is then

$$F = \int_V f + \kappa(\nabla c)^2 dV, \quad (1)$$

where  $f$  is the bulk free energy density and  $\kappa$  is a constant. We expect that the system will be unstable to small fluctuations in concentration with respect to the mean concentration  $c'$ ,  $(c - c') = \delta c = a \sin(\mathbf{k} \cdot \mathbf{r})$ . Here the wavevector  $k = 2\pi/\lambda_{\text{spin}}$  with  $\lambda_{\text{spin}}$  a characteristic lengthscale.

Expanding the free energy density about  $c'$  we have

$$f(c) \approx f(c') + (c - c') \frac{\partial f}{\partial c} \Big|_{c=c'} + \frac{1}{2}(c - c')^2 \frac{\partial^2 f}{\partial c^2} \Big|_{c=c'} + \dots \quad (2)$$

The integrand in equation (1) is then

$$\begin{aligned} f(c) + \kappa(\nabla c)^2 &\approx f(c') + a \sin(\mathbf{k} \cdot \mathbf{r}) \frac{\partial f}{\partial c} \Big|_{c=c'} \\ &\quad + \frac{1}{2} a^2 \sin^2(\mathbf{k} \cdot \mathbf{r}) \frac{\partial^2 f}{\partial c^2} \Big|_{c=c'} + a^2 \kappa^2 \sin(\mathbf{k} \cdot \mathbf{r}) + \dots \end{aligned} \quad (3)$$

If we now integrate to obtain the change in free energy over the whole system, we have

$$\frac{\delta F}{V} = \frac{a^2}{4} \left[ \frac{\partial^2 f}{\partial c^2} \Big|_{c=c'} + 2\kappa^2 \right]. \quad (4)$$

Thermodynamic stability requires that the term inside the square brackets is positive. So for instability, i.e. spinodal decomposition, we identify a critical (maximum) wavevector

$$k^c = \sqrt{-\frac{1}{2\kappa} \frac{\partial^2 f}{\partial c^2} \Big|_{c=c'}} \quad (5)$$

and corresponding lengthscale  $\lambda^c = 2\pi/k^c$ . What this tells us is that for lengthscales above  $\lambda^c$ , fluctuations are *unstable*. Now if we consider diffusion we can obtain a fastest growing lengthscale (see figure 3). We can also obtain the rate of change of concentration as a function of time which corresponds to that lengthscale. The diffusion equation  $\partial c/\partial t = M\nabla^2\mu$  where  $M$  is a constant and the chemical potential in Cahn–Hilliard theory

$$\mu = \frac{\partial F}{\partial c} = \frac{\partial f}{\partial c} \Big|_{c=c'} - 2\kappa\nabla^2 c. \quad (6)$$

We can then relate the free energy density to the rate of change of concentration

$$\frac{\partial c}{\partial t} = M \left[ \frac{\partial f}{\partial c} \Big|_{c=c'} \nabla^2 c + 2\kappa\nabla^4 c \right] \quad (7)$$

and as before consider a concentration fluctuation now with a time-dependent component  $\delta c = a \exp(\omega t) \sin(\mathbf{k} \cdot \mathbf{r})$ . From equation (7) and dividing by  $\delta c$  we have

$$\omega = M \left[ -\frac{\partial f}{\partial c} \Big|_{c=c'} k^2 c + \kappa k^4 \right]. \quad (8)$$

We arrive at a wavevector for the fastest growing fluctuations as

$$k^{\text{spin}} = \sqrt{-\frac{1}{8\kappa} \frac{\partial^2 f}{\partial c^2} \Big|_{c=c'}} \quad (9)$$

and corresponding lengthscale  $\lambda^{\text{spin}} = 2\pi/k^{\text{spin}}$ . Therefore, at short timescales, domains of  $\lambda^{\text{spin}}$  increase in colloid volume fraction with growth rate related to  $\partial c/\partial t = \omega$ . For *arrested* spinodal decomposition, once the volume fraction in the colloid-rich regime is  $\phi_c \approx 0.6$ , the system undergoes dynamical arrest (see section 2.2 and figure 4(a)) [66, 77–79]. This need not be the case, as larger polymer–colloid size ratios lead to colloidal liquids for which  $\phi_c < 0.6$ , and phase separation proceeds to completion (figure 3). In this case, at longer

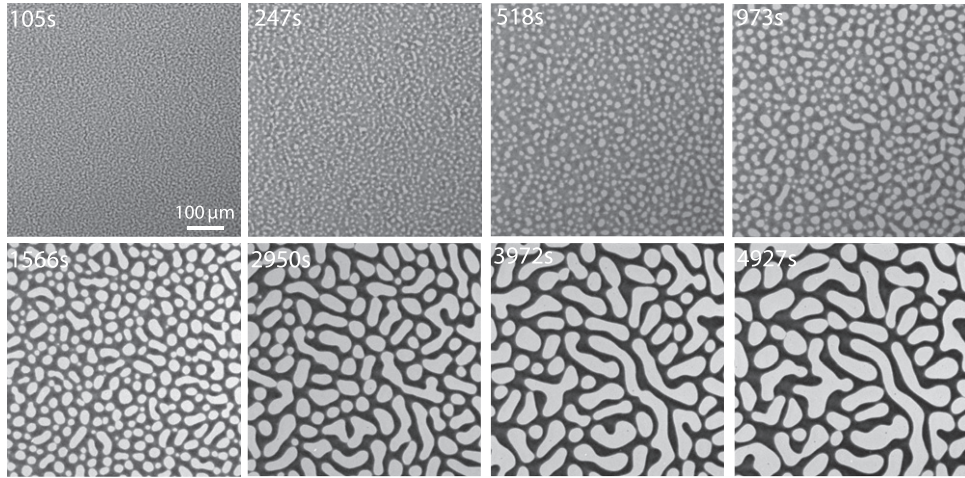


**Figure 3.** Confocal microscopy data of a colloid–polymer mixture undergoing spinodal decomposition without arrest. Here the polymer–colloid size ratio is around  $q = 2.5$ , i.e. the polymers are larger than the colloids. The colloidal liquid does not reach volume fractions at which arrest sets in and phase separation proceeds. The early stage of spinodal decomposition (as described by equations (1)–(5)) is approached in the first two panels. Later stages with coarsening are shown panels corresponding to longer times. Reprinted from [81], with the permission of AIP Publishing.

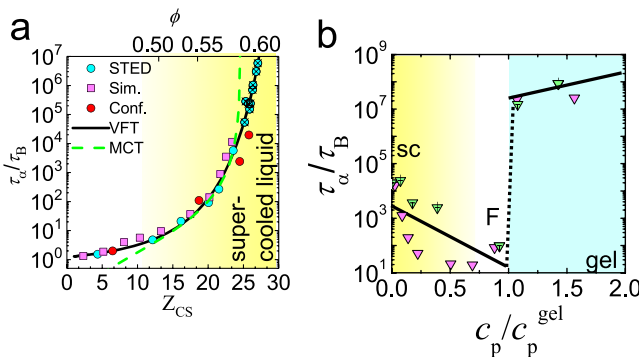


**Figure 4.** Differences in dynamical arrest between vitrification and gelation. (a) The glass transition in hard-sphere colloids. Here  $Z_{CS}$  is the compressibility factor according to the Carnahan–Starling equation of state. Increasing the volume fraction leads to a *continuous* increase in relaxation time from the colloidal fluid (F) to the supercooled liquid (SC). Here VFT is a fit with the Vogel–Fulcher–Tamman equation (equation (10)), red and blue data are from particle-resolved experiments and pink are computer simulation. Reproduced from [94]. CC BY 4.0. (b) Gelation. The fluid to gel transition is abrupt, as the system passes through the spinodal line to form the gel (see figure 2). Note that there is also some acceleration for small polymer concentration, this is thought to be due to cage-opening [47]. Pink data are computer simulation, green are particle-resolved experiments. Reprinted from [48], with the permission of AIP Publishing.

timescales, the network coarsens following a power-law  $\lambda \sim t^n$  where the power  $n$  depends on the particular dynamics of the system.

## 2.2. The colloidal glass transition in the context of spinodal gelation

Central to the emergence of solidity in colloidal gels is the glass transition that occurs upon densification of the ‘colloidal liquid’ phase of the demixing system. We have noted that the colloidal liquid undergoes densification under spinodal decomposition. In colloid–polymer mixtures, partition of the colloids and polymers is such that the colloid-rich phase is

largely devoid of polymers. Of course the polymer chemical potential (or, osmotic pressure) is taken to be equal in both phases [24]. However it is nevertheless tempting to view the arrest of the colloid-rich phase as being similar to the glass transition in hard spheres<sup>8</sup>, and indeed it is hard to avoid the conclusion that the arrest is driven by the steric effects of the colloids. However it is important to note that in a gel of course there are interfaces between colloid-rich and colloid-poor phases and this is likely where the majority of the particle motion takes place (see section 5.1) [55, 83–86].

As noted above, the glass transition is a challenge, but one which real space analysis of colloidal hard spheres is amenable to [48, 87–89]. Before reviewing some contributions, we give the briefest of outlines of what we consider to be the state of the art. The glass transition is a *scientific revolution* as introduced by Kuhn [90]. That is to say, there are interpretations (or theories, depending on one’s position), which start from *fundamentally different standpoints*, and yet which describe the available data equally well. It is far beyond the remit of this review of real space analysis of colloidal gels to address the glass transition, other than to give reference to some of the many reviews [58, 69, 71] and shorter perspectives [72–75] of the glass transition. The best-known first-principles theory, mode-coupling theory (MCT) describes the first 4–5 decades of increase in relaxation time (or viscosity) [91, 92]. However, at deeper supercooling, (higher volume fraction in the case of colloids), it has been shown e.g. in (figure 4(a)) that although MCT in its conventional form predicts a transition to a solid with infinite relaxation time, in practice relaxation *does* occur, through mechanisms not captured by MCT [89, 93, 94]. MCT can be improved, to remove some of the approximations by

<sup>8</sup> While the discovery of the ‘attractive glass’ [47] has received much attention, in fact it has recently been shown that while adding attraction to hard spheres does initially accelerate a supercooled hard sphere fluid, but arrest under further attraction is interrupted by gelation for volume fractions at least up to  $\phi \approx 0.6$  [48, 82].

considering higher-order correlations [95], but we are some way from viewing it as a full description.

Mechanisms for the relaxation at deeper supercooling (or higher volume fraction in the case of colloidal hard sphere-like systems) postulated by theories such as Adam–Gibbs theory [96] random first-order theory [97], replica theory [76, 98], and geometric frustration [99] are (like MCT) based on thermodynamic principles but are highly approximate. Other interpretations such as dynamic facilitation postulate that it is the dynamical behaviour of the system (not the thermodynamics) which drives arrest [100]. It has been suggested that these seemingly disparate approaches built on either thermodynamics [76, 91, 92, 96–99] or dynamics [100] may in fact be reconciled [75, 101].

To summarise, it is fair to say that for the purposes of colloidal gelation, colloids at high density may be treated as a viscoelastic system, that is to say, a material that is solid-like on short timescales but ultimately flowing at sufficiently long timescales. It is worth noting that the structural relaxation time  $\tau_\alpha$  or viscosity of hard-sphere-like colloidal systems increases *continuously* in response to increasing the volume fraction. This, along with the deviation from MCT, is plotted in figure 4(a). These data are well-fitted by the celebrated Vogel–Fulcher–Tammann (VFT) ‘law’

$$\tau_\alpha(\phi) = \tau_\infty \exp\left[\frac{A}{(\phi_0 - \phi)^\delta}\right], \quad (10)$$

where  $\tau_\infty$  is the relaxation time in a dilute system,  $\phi_0$  is the point at which the relaxation time would diverge,  $A$  is a measure of the fragility and  $\delta$  is an exponent typically set to one to recover the conventional VFT form. The VFT form has *some* theoretical justification [69], but is far from the only choice, [102, 103], although the VFT fit in figure 4 is clearly better than MCT.

At the end of this section, we identify four characteristics of spinodal gelation [1, 5, 28]. (i) The system must undergo spinodal decomposition; (ii) there must be *dynamic asymmetry* between the phases (that is to say, one phase is substantially more viscous than the other) [1]; (iii) the more viscous phase must percolate [104]; (iv) the non-equilibrium nature of the gel leads to ageing, in particular coarsening.

### 2.3. The quest for a theory of gelation

This continuous increase in viscosity in vitrification is very different from that of gelation, where the viscosity of the material increases abruptly as the gelation line (the spinodal) is traversed (figure 4(b)) following the path indicated in figure 2 [48]. This is significant, as it emphasises that the glass transition and spinodal gelation are fundamentally different phenomena. One would therefore not expect the same theory to describe both and indeed while it is possible to use advanced liquid state theories to predict the structure of colloidal fluid approaching gelation [52] and mode coupling theory to predict dynamical arrest upon increasing attraction between colloids [50], it is unclear that this is really referring to gelation, as the phase separation is not included by default [48].

We emphasise that gelation via spinodal decomposition is far from the only class of gelation [3, 5]. It forms our focus here because the vast majority of real space studies of colloidal gelation pertain to spinodal gelation. Other standpoints have been put forward including cluster growth [105], a glass transition of ramified clusters [106] and an emphasis has been placed on percolation [107]. In the case of the latter, dynamical arrest was associated with an inferred percolation line in a rheological study [107]. The relation between percolation and gelation was subsequently probed in real space (figure 2) and also in computer simulation, where no change in dynamics at percolation was found [48]. This is consistent with fluids of, e.g. square well particles whose second virial coefficient is insufficient for gelation (see below [78]), which can be prepared a volume fractions up to  $\phi \lesssim 0.58$  without undergoing arrest which of course percolate if one considers the interactions between the particles to constitute a bond. In other words, percolation is a necessary but insufficient condition for gelation. It is possible that the system studied previously [107] may perhaps have had some additional interactions which might have complicated the situation.

An emphasis has been laid on cluster growth in the approach to gelation [108] and analogies with the sol–gel transition have been made, lengthscales intermediate between single-particle (microscopic) and macroscopic have been considered. Very recently, gelation has been associated with a non-equilibrium percolation transition [39, 40]. This is an interesting perspective, playing as it does to particle-level analysis, and is likely to be broadly compatible with the spinodal decomposition mechanism (see section 4.1 and figure 2).

As it stands, while a number of approaches are being pursued [50, 51, 53, 54, 108, 109] theoretical understanding of gelation beyond that outlined here is rather limited, with motivation for future work. Furthermore, this discussion pertains to the process of gelation, the emergence of solidity. The failure of gels under gravity, or external loading is an exciting and challenging research area. Concerning the response of soft materials to external loading, we direct the reader to some excellent reviews [110–113].

## 3. Brief overview of (effective) attractions between colloidal particles

Here we mention some interactions specific to the formation of colloidal gels, and in particular we discuss certain factors pertinent to the work reviewed in the later sections. Interactions between colloids are detailed in a number of textbooks, e.g. [43].

*Van der Waals interactions.*—The van der Waals interactions between colloids result from the sum of these interactions between the constituent molecules, and may be taken to have a  $1/r^6$  form,

$$u_{vdW}(r) = -\frac{C\rho_1\rho_2}{r^6}, \quad (11)$$

where  $C$  is a constant, and  $\rho_{1,2}$  is the number density of molecules in colloids 1 and 2. Integrating over the colloids of

volumes  $V_{1,2}$  then yields

$$u_{vdW}(r) = - \int_{V_1} dV_1 \int_{V_2} dV_2 \frac{C\rho_1\rho_2}{r^6}. \quad (12)$$

In the case of two spherical colloids of radii  $a_1$  and  $a_2$ , we have

$$\begin{aligned} u_{vdW}(r) = & -\frac{A}{3} \left\{ \frac{a_1 a_2}{r^2 - (a_1 + a_2)^2} + \frac{a_1 a_2}{r^2 - (a_1 - a_2)^2} \right. \\ & \left. + \frac{1}{2} \ln \left( \frac{r^2 - (a_1 + a_2)^2}{r^2 - (a_1 - a_2)^2} \right) \right\}, \end{aligned} \quad (13)$$

where  $A = \pi^2 C \rho_1 \rho_2$  is the Hammaker constant. For colloids close together, such that the separation of their surfaces  $h = r - (a_1 + a_2) \ll \min(a_1, a_2)$

$$u_{vdW}(h) \approx -\frac{A}{6h} \frac{a_1 a_2}{a_1 + a_2}. \quad (14)$$

**Refractive index matching.**—Typically the van der Waals interactions between two colloids at contact are thousands of times the thermal energy and result in irreversible aggregation of colloids, if the electrostatic repulsions between the particles are sufficiently screened by the addition of salt. However, refractive index matching of colloids and solvent changes all that. The constant  $C$  is related to the (mean) polarisability  $\alpha$  of the constituent molecules, which is related to the refractive index  $n$  through the Lorentz–Lorenz equation

$$\frac{n^2 - 1}{n^2 + 2} = \frac{4\pi}{3} \rho \alpha, \quad (15)$$

where  $\rho$  is now averaged. Thus, if the colloids and the solvent have the same refractive index, the net force on the particles will sum to zero and the van der Waals contribution will vanish. In practice, refractive index matching of solvent and colloids is sufficient that the residual van der Waals interactions are a small fraction of  $k_B T$  and can often be neglected.

**The depletion interaction.**—In addition to the short-ranged van der Waals interaction mentioned above, in multispecies colloidal mixtures attraction can be caused by the depletion interaction. This was first introduced by Asakura and Oosawa (AO) [31] and rediscovered by Long and co-workers [32]. This depletion interaction is driven by the entropy of the smaller species which can either be colloids or polymers. In the latter case a reasonable approximation is found, so that the polymers are treated as ideal and one can formally integrate them out [114]. This AO model leads to an effective pair interaction between two hard colloidal spheres in a solution of ideal polymers, which is illustrated in figure 5(a).

$$\beta u_{AO}(r) = \begin{cases} \infty & \text{for } r < \sigma \\ \frac{\pi(2R_G)^3 z_p^r}{6} \frac{(1+q)^3}{q^3} \\ \times \left\{ 1 - \frac{3r}{2(1+q)\sigma} + \frac{r^3}{2(1+q)^3 \sigma^3} \right\} & \text{for } r \geq \sigma < \sigma_C + (2R_G) \\ 0 & \text{for } r \geq \sigma + (2R_G), \end{cases} \quad (16)$$

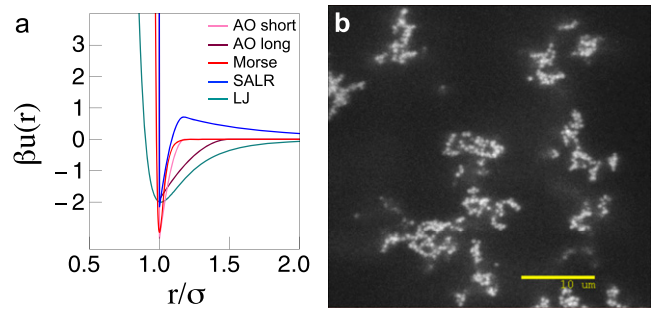


**Figure 5.** (a) Spherically symmetric interactions between colloids pertinent to gelation. The AO interaction is shown for a short range ( $q = 0.18$ ) system where the colloidal liquid is not thermodynamically stable (pink) and a longer range ( $q = 0.5$ ) where the liquid is stable (maroon). Also shown is the Morse interaction for range parameter  $\rho_0 = 33$  (red) and Lennard-Jones interaction (teal). Finally a competing interaction which is the sum of a short-ranged attraction and long-ranged repulsion (SALR, blue), as postulated for gelation in the density matched PMMA system (see section 4.1). (b) Early particle-resolved confocal microscopy image of a colloidal gel. Density matched PMMA colloids with diameter  $\sigma = 1500$  nm and polystyrene polymer with size ratio  $q = 0.11$  and colloid volume fraction  $\phi_c = 0.03$ . Bar = 10  $\mu\text{m}$ . Reproduced from [117]. © IOP Publishing Ltd. All rights reserved.

where  $\beta = 1/k_B T$ ,  $R_G$  is the polymer radius of gyration and the polymer–colloid size ratio  $q = 2R_G/\sigma$ , the polymer fugacity  $z_p^r$  is equal to the number density  $\rho_p^r$  of ideal polymers in a reservoir at the same chemical potential as the colloid–polymer mixture. Thus, because the prefactor is proportional to the polymer reservoir concentration, the effective temperature is inversely proportional to the polymer reservoir concentration. The result is an effective interaction between the colloids of range  $q\sigma$  and well-depth  $u_{AO}^{\min}$ . For  $q \leq 0.1547$  it is formally accurate, in the sense that many-body effects due to integrating out the polymer degrees of freedom are absent [114, 115]. The Morse interaction is a useful, variable ranged attractive interaction which reproduces very well the AO interaction as shown in figure 5(a).

$$\begin{aligned} \beta u_{Morse}(r) = & \beta \varepsilon_{Morse} \exp [\rho_0 (1 - r/\sigma)] \\ & \times (\exp [\rho_0 (1 - r/\sigma)] - 2). \end{aligned} \quad (17)$$

In fact, for some parameters, the Morse interaction appears to reproduce the higher order structure of colloidal fluids better than the one-component AO interaction [116].

#### 4. Real space analysis

Here we take real space analysis to pertain to microscope-based studies of colloidal systems. *Particle-resolved studies* is then a subset of real space analysis where the individual colloidal particles are visible [43] and in which the coordinates of colloidal particles may be obtained [43, 118–120]. Particle-resolved studies have had a major impact in a number of fields since their inception in the pioneering and far-sighted work of van Blaaderen and co-workers [87, 121]. Such areas include the glass transition [87, 88] and crystal nucleation [122, 123]. Crucial to this breakthrough was the use of a confocal microscope, to enable 3D optical imaging and a colloidal system

whose particles were sufficiently large and which were refractive index matched to the solvent. The advent of coordinate tracking algorithms [124–127] meant that the 3D coordinates of the particles could be extracted. In some cases, it is even possible for the *diameter* of every particle to be obtained, which is useful in the case of polydisperse systems [128]. The technique of particle-resolved studies has been extensively reviewed previously [43, 118, 119]. We refer the reader to those reviews and now focus the use of real space analysis in colloidal gelation.

#### 4.1. Early work and the mysteries of electrostatics in density-refractive index matched colloids

The first use of 3D real space analysis for colloidal crystallisation driven by depletion attractions appears to be that of Koen derink *et al*, who used silica rods as the depleting agent [129]. Note that silica is typically not density matched, due to its high density. Indeed to our knowledge, this has only been achieved with a highly volatile solvent [130]. De Hoog *et al* carried out pioneering particle-resolved studies in a refractive index and (nearly) density matched system with depletion interactions, revealing the interplay between self-assembly and geometric frustration [131]. This was followed by Dinsmore and Weitz [117], which we understand to be the first particle-level structural characterisation of a colloidal gel. The system considered was the poly-methyl methacrylate (PMMA) colloids with polystyrene polymer in a refractive index and (mass) density-matching solvent. This system, with some variants, has been used extensively since, and some comments are in order.

PMMA colloids were used to mimic hard spheres in the seminal work of Pusey and van Megen [132]. The thin ( $\sim 5\text{--}10\text{ nm}$  [133, 134]) layer of steric stabilisation afforded a degree of softness small in comparison to the diameter of the particles (typically around 400 nm). That and later work which used light scattering for structural analysis of the system was able to use smaller colloids, where the effect of gravity was relatively small. The effect of gravity may be quantified via the gravitational length, which is the height that a colloid may be raised such that the gravitational potential energy is equal to the thermal energy  $k_B T$ ,  $\lambda_g = k_B T / (\delta\rho\pi\sigma^3 g/6)$  where  $\delta\rho$  is the mass density difference between the solvent and the colloids and  $\sigma$  is the colloid diameter. Substituting typical values in (assuming that the solvent is the commonly used *cis*-decalin, whose density is less than that of PMMA), we find a gravitational length of around  $100\sigma$  for 400 nm diameter particles.

However, particle resolved studies requires larger colloids of  $2\text{--}3\ \mu\text{m}$  if the coordinates are to be tracked [43]. In the *same solvent* considering the gravitational length *in units of the colloid diameter*, we have a gravitational length of just  $0.03\sigma$ , putting such  $3\ \mu\text{m}$  particles firmly in the regime of granular matter where the effects of gravity dominate the thermal energy. Clearly, something must be done to reduce the effects of gravity if these larger particles are to behave as colloids and be dominated by the thermal energy. The solution was to match the density of the solvent and particles, by mixing two solvents together, for example adding cyclo-hexyl bromide (whose density is greater than that of PMMA, and whose refractive index is, like that of *cis*-decalin, conveniently close

to that of PMMA), then the  $\delta\rho$  term becomes small and colloidal behaviour is regained with  $\lambda_g \gg \sigma$ . It is worth noting that *perfect density matching is not possible*, due for example to the different thermal expansivities of the PMMA colloids and the solvent mixture, and the inevitable temperature fluctuations that occur during experiments. Good density matching might correspond to a gravitational length of (say)  $\sim 100\sigma$  [135].

Although the sedimentation issues of the larger PMMA colloids were resolved by using the cyclo-hexyl bromide (CHB)-*cis*-decalin solvent mixture, the larger particles behaved in a manner very unlike the earlier work with smaller sub-micron colloids. The reason for this was the fact that the electrostatic charge borne by the larger PMMA colloids was sufficient to massively change the phase behaviour. The cause for the electrostatics becoming significant is two-fold: firstly the solvent is different: the dielectric constant of the density matching CHB-*cis*-decalin mixture is 5.37, while that of *cis*-decalin alone is 2.4 [136]. Although ion dissociation is weak in the density matching mixture, it is very much more than in pure *cis*-decalin, and indeed the solvents used in the early work with light-scattering of small particles had dielectric constants around 2, in which there is less ion dissociation with respect to the CHB-*cis*-decalin density matching mixture. Secondly, the particles are much larger. If we make the not entirely unreasonable assumption that the surface charge per unit area is fixed, then an increase in particle size from 400 nm to  $3\ \mu\text{m}$  corresponds to an increase in surface area by a factor of 56. Given that the electrostatic interaction scales with the *square* of the charge it is clear that the electrostatic interactions would be very much stronger. For example, if we consider the case of a 400 nm colloid system with 7 electronic charges per colloid and Debye length of 1 micron, this would have a contact potential of  $k_B T$  with little effect upon phase behaviour. A 3 micron colloid, in the same solvent with the same Debye length with a similar surface charge density would have a carry a charge of 415, corresponding to a contact potential of around  $100k_B T$ —which is substantially larger than any attraction driven by depletion, so there *should* be no gelation at all [137, 138]. Moreover in the lower dielectric constant solvents used previously with the smaller colloids, the charge carried on each colloid would be even less than seven elementary charges and often safely neglected. While some experiments on colloids in micro-gravity have been carried out (using techniques other than particle-resolved studies) [77], it is hard to see how a confocal microscope would survive a launch in order to be operated in space, so for now, particle-resolved studies remains earthbound. This need not mark the end of the story. For example it has been shown that by simulating microgravity on Earth through slow rotation, that sedimentation can be suppressed [139].

In retrospect, then, we can see that while Pusey and van Megen found excellent agreement with hard sphere like behaviour with 400 nm colloids in a solvent with dielectric constant around 2 [132], Yethiraj and van Blaaderen [142] found that the larger PMMA crystallised at a volume fraction  $\phi \lesssim 0.01$ , some 50 times less than hard spheres [136, 143], and Wigner glasses (dynamical arrest driven by electrostatics)

have been found at similar volume fractions  $\sim 0.01$  [137]. The effects of such electrostatic behaviour have been reviewed in some detail [134, 138], but before leaving this topic we note that the interaction of these nonaqueous systems with water can be very complex [144], and depends on the amount of water the system comes into contact with. What this means is that even the same system may not exhibit the same behaviour, if environmental factors, like the humidity, change. For now we note that electrostatic interactions can have a profound, complex and sometimes uncontrollable, effect upon real space analysis of gelation in colloids.

In applying the then newly-developed density-matched, refractive index-matched PMMA–CHB–*cis*-decalin system to gelation, the work of Dinsmore and Weitz [117] demonstrated the power of particle-resolved studies. The characteristics of colloidal gels, the fractal dimension, mass distribution of clusters and neighbour distributions were obtained. Also, local measures, inaccessible to bulk techniques such as scattering, like the chain topology and the number of pivots for each particle in an ‘arm’ of a gel were found. Soon after, the same lab exploited the effect of the range of the depletion interaction: small polymers ( $R_G \approx 6$  nm) lead to very short-ranged attractions (equation (16)) which are of the same order as the stabiliser layer on the PMMA colloids. This suppresses the rotation of the colloids around one another, presumably as the stabiliser ‘hairs’ would interdigitate. Longer ranged interactions with ( $R_G \approx 35$ ) nm led to structures consistent with the particles rotating around each other. Thus it is possible to include an angular dependence into a depletion interaction through a judicious choice of polymer size [145]. We note that surface roughness has been explored to considerable effect in the elegant work of Zhao and Mason [146].

The work of Dinsmore and Weitz was followed from the same lab, by Lu *et al*’s work on clusters [147]. This demonstrated a truly exceptional degree of density matching, as clusters of hundreds or even thousands of particles were studied. Given the discussion above, to density match such large assemblies (of already rather large colloids), represented a truly Herculean task of exquisite control over the sample preparation and experimental conditions. Lu *et al* used a large amount of salt to screen the electrostatics. While Yethiraj and van Blaaderen [142] had demonstrated the use of salt to screen the electrostatic interactions, they used relatively small quantities, and indeed it was later determined by Leunissen and co-workers that the saturation concentration of the tetrabutyl ammonium bromide (TBAB) salt often used is a mere 260 nM [136, 148]. At this salt concentration, the Debye length ( $\approx 100$  nm) is similar to the range of the depletion interaction and the electrostatics strongly influence gelation [149]. Lu *et al* used 4 mM of the same salt, and it is possible that, due to the low ionic strength and slow approach to equilibrium in these systems [136] some non-equilibrium salt concentrations above the 260 nM were possible. While ion-dependent non-equilibrium phenomena might seem surprising, given that small ions ‘should’ relax in the timescale of picoseconds, over a timescale of hours to days, a variety of *peculiar, time-dependent phenomena* have been observed: the low density crystals noted above melt [136, 143] and clusters in

the ‘mermaid-like’ systems undergo electrostatically-induced fission [137]. In any case, Lu *et al*’s work found good agreement with expectations from theory (e.g. [24, 114]), except that the clusters observed would be expected to be a metastable state, with the equilibrium being a (colloidal) gas-crystal phase coexistence. It is worth noting that the approach to equilibrium for such a system can be extremely slow, in principle running to years or more [19].

An important advance around this time was to explicitly investigate the interplay of solvent composition (and density matching) and electrostatics, by Sedgwick *et al* [140]. It is clear from the discussion above that this is an important issue, and three scenarios were considered. The first used a pure *cis*-decalin solvent, which was not density matched but the behaviour was otherwise consistent with expectations. The second case was to consider a density-matched solvent but with added salt, which was also found to be consistent with expectations. The third case where no salt was added was more intriguing as although gels were formed, more polymer was needed than in the case where the electrostatics were screened. This was not surprising, because now the stronger, unscreened electrostatic repulsions needed to be overcome for aggregation, but what was intriguing was the observation of *elongated* clusters (figure 6(a)). These were interpreted as being a result of the electrostatic repulsions [150], and indeed similar behaviour was observed in Lysozyme protein solutions, where the attractions came from van der Waals interactions between the protein molecules [151]. For proteins, it is important to emphasise that while some observations are possible with real space analysis using optical microscopy (see section 7 [14]), we required techniques such as x-ray scattering to probe the lengthscales appropriate to interactions between protein molecules [152–155]. Indeed, x-ray scattering was used to infer the protein clusters in question, however the results were later disputed [156]. It is worth noting that while such spherically symmetric short-range attraction—long-range repulsion (or ‘mermaid’) interactions (figure 5(a)) are a simple model for protein–protein interactions, in reality the situation is far more complex, due not least to the relatively small number of discrete charged sites on the protein and side-chains [12, 14, 157].

Unlike the protein clusters, due to the larger size of the particles, the elongated colloidal clusters were clearly visible in the confocal images in figure 6(a). Gels of such particles with these ‘mermaid’ interactions were even shown to be resistant to gravitational collapse (section 5.3) [158]. However the behaviour of the electrostatic interactions in this and other work [137, 141, 149, 159] have been analysed in some detail. In the case that the electrostatics are strongly screened through the addition of salt [149, 160], behaviour consistent with a superposition of attractive (depletion) and repulsive (electrostatic) contributions can be realised. However in this case the range of the electrostatic interactions is comparable to, or less than, the depletion-induced attractions. In the case that the screening is weak, such that the electrostatic repulsions are longer-ranged than the attractions a breakdown in spherical symmetry of the interactions has been identified [138, 159], not to mention large inconsistencies in the calculated strengths

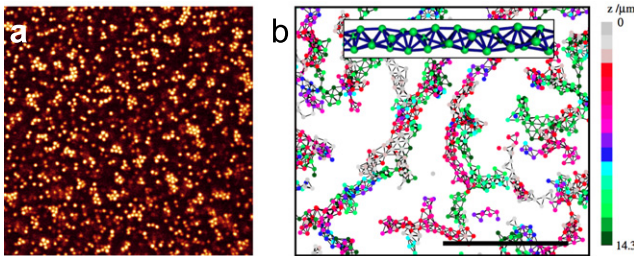


**Figure 6.** Indications of ‘mermaid-like’ interactions in clusters and gels. (a) A confocal micrograph of the clusters in a sample with volume fraction  $\phi = 0.086$  and polymer concentration  $c_p = 3 \text{ mg cm}^3 q = 0.021$ . Here the colloids had a diameter of 1320 nm. Note the spacing between the monomers, indicating a significant strength and range of the repulsive interactions. Reproduced from [140]. © IOP Publishing Ltd. All rights reserved. (b) A two-dimensional projection of the particle centres within a slab of gel in a colloidal system with competing interactions. Particles are coloured as a function of their depth within the sample and drawn 40% of their actual size for clarity. Inset: a spiral chain formed from tetrahedra of particles sharing faces. Reprinted (figure) with permission from [141], Copyright (2005) by the American Physical Society.

of the attractive and repulsive components [137, 138]. Even in the case that the dielectric constant is around 2 through a suitable choice of solvents, so that electrostatic interactions are small, surprises can still occur [159]. In the multicomponent index and density matching solvents used, one or other component can be absorbed by the colloids and this breaks the refractive index matching, leading (in addition to poor imaging) to significant van der Waals attractions between the colloids [134, 161].

Other work showed fascinating Bernal spirals (figure 6(b)) [141] which were attributed to the interplay between long-ranged electrostatics and polymer-induced depletion attractions. These spirals were subsequently reproduced by computer simulation [162], although the experimental system likely exhibited the breakdown in spherical symmetry of the interactions noted above.

The interplay of electrostatics and depletion in the PMMA system continues to arouse interest. Recently, Kohl *et al* suggested that *directed* percolation, in which percolation occurs through steps through the network only in a preferred direction could be identified in gelation of the charged PMMA system [163]. This was curious, as there is no obvious reason for the symmetry breaking implicit in a preferred direction for directed percolation. Percolation (that is to say, un-directed percolation) had previously been linked to gelation [164], but subsequent work has shown that while percolation is a necessary condition for gelation, no change in dynamical behaviour could be identified upon percolation [48]. The same holds for directed percolation which occurs at higher colloid volume fraction than does (undirected) percolation, but there was found to be no change in dynamical behaviour at the directed percolation transition [165].

#### 4.2. Evidence for spinodal decomposition as a mechanism for gelation

While we have assumed that spinodal decomposition is the mechanism by which a colloid-rich network is formed (the

beginnings of phase separation), and local dynamical *arrest* prevents gels of ‘sticky spheres’ from fully phase separating, in fact we have provided little hard evidence in that direction. Spinodal decomposition had been proposed for some time [64–66, 77], but was not the only proposed mechanism, others included MCT [50] and arrest of fractal clusters [106], along with cluster aggregation [39, 105]. It is fair to say that the *tour de force* of Lu *et al* in 2008 [78, 79] provided, if not unequivocal proof then very compelling evidence in support of spinodal decomposition. In an ingenious approach, they mapped the experimental PMMA with salt system onto the square well interaction potential, whose phase diagram is well known. Now there are various ways to map colloidal systems onto well-known models [133, 134, 136], but it is often challenging and confounded by poorly controlled phenomena like electrostatics (see above) [138]. The method employed here was novel and elegant: the size distribution of clusters in the ergodic fluid phase was compared between simulation and experiment and from this equivalent state points were identified as shown in figure 7. This mapping of equivalent state points enabled the reduced second viral coefficient  $B_2^*$  to be determined in the experiment (it can readily be calculated for the simulation). It is known that we expect spinodal decomposition for the square well system for  $B_2^* \approx 3/2$  [166],<sup>9</sup> and this is precisely what Lu *et al* found. They were also able to use their particle-resolved data to measure the volume fraction of the dense phase for the first time and arrived at a value of  $\phi_c = 0.60$ , certainly sufficient for dynamical arrest (see figure 4(a)) [48]. The strength in Lu *et al*’s work lay at least in part in its precision: at the very attraction strength at which phase separation and spinodal decomposition is expected, is when gelation is observed. Later work showed that the dynamics change abruptly at the point of gelation figure 4(b) [48]. This does not mean that other mechanisms do not contribute and particularly at low volume fractions, there is strong evidence for the role of cluster growth [77, 80] (see also the discussion in section 5.1). However such clusters almost certainly lie within the region of the phase diagram where spinodal demixing occurs, with percolation taking longer to occur at these low volume fractions (see the pale blue region where cluster growth is important in figure 2). Percolation is of course a necessary (but insufficient) condition for gelation [104].

One may enquire as to the nature of gelation (if any) of systems in which spinodal decomposition does not occur. In a most elegant work, Bianchi *et al* showed that by reducing the ‘valency’ of colloidal particles, the liquid–gas transition can be suppressed to low volume fraction [21]. Such *empty liquids* thus enable attraction-driven arrest without spinodal decomposition intervening. As shown schematically in figure 8 one may ‘quench’ the system by increasing the attraction strength higher volume fraction than the liquid–gas binodal and spinodal decomposition is avoided. It has been shown that under

<sup>9</sup> Strictly this holds only at criticality, however the spinodal of the square well system for these short interaction ranges is so flat, that for practical purposes the same interaction strength induces gelation for off-critical colloid volume fractions also [48].

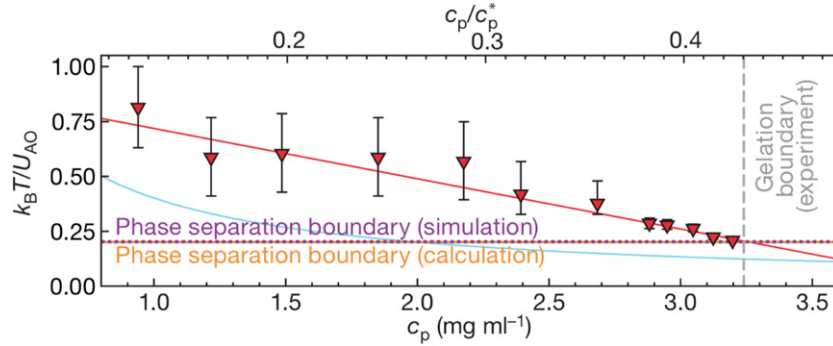


**Figure 7.** Mapping interactions in particle-resolved experiments to computer simulation using cluster size distributions. Note that the measured gel point coincides precisely with that predicted for the system to undergo phase separation. Reprinted by permission from Springer Nature Customer Service Centre GmbH: [Springer Nature] [Nature] [78] (2008).

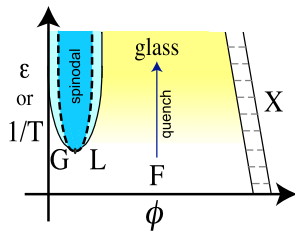


**Figure 8.** Schematic of inducing dynamical arrest in ‘empty liquids’ via increasing the attraction strength. An ergodic fluid with weak interactions will exhibit progressively slower dynamics (yellow shaded region) upon an increase in the attraction strength (blue arrow marked ‘quench’). By passing to the high-density side of the liquid–gas phase separation (which occurs at very low volume fraction in ‘empty liquids’) spinodal decomposition is bypassed. The dynamics are expected slow in a manner than is Arrhenius (or close to Arrhenius) [20], consistent with strong glassforming systems like silica [70]. This is quite unlike the drastic change upon crossing the spinodal (figure 4(b)). Such a continuous increase in the structural relaxation time is indistinguishable from vitrification from a thermodynamic point of view [48].

such conditions, the increase in structural relaxation time is continuous and gradual [20], quite unlike the drastic increase in structural relaxation time that occurs in the case of spinodal gelation (figure 4(b)). In fact, such systems are thermodynamically indistinguishable from strong glasses formed from network glassformers like silica [20, 58, 70], and thus in a sense, are not gels at all—unless we recast most famous glass of all as a gel!

#### 4.3. A local mechanism for arrested spinodal decomposition

The mechanism of dynamical arrest in glasses, and, by implication, colloidal gels, has long confounded our understanding, as discussed in section 2.2. Among the key challenges is the noted perceived wisdom that *the microscopic structure underlies the macroscopic behaviour* [44]. The near-absence of any change in the two-point structure (for example the static structure factor) in atomic and molecular [70] or colloidal [167] systems approaching the glass transition thus presented a challenge. Higher-order correlation functions, for example three-body correlations or geometric motifs such as the icosahedra originally proposed by Sir Charles Frank, due to their low potential energy with respect to crystalline structures [168] and

later incorporated in the theory of geometric frustration by Tarjus and co-workers [99] are hard, though not impossible [70] to identify in atomic and molecular systems.

However, in particle-resolved studies, access to higher-order correlation functions is afforded by the particle coordinates, which was recognised by van Blaaderen and Wiltzius [87], in their determination of the Steinhardt bond-orientational order parameter  $W_6$  [169], whose negative value was interpreted as evidence for fivefold symmetry, consistent with the conjecture of Frank [168]. Some of us built on Frank’s ideas and applied them to colloidal gelation. Frank’s conjecture was that because the icosahedron was the minimum energy structure for 13 Lennard-Jones atoms *and* because a common coordination number in bulk liquids is 12, one should expect such geometric motifs in supercooled liquids. It was therefore tempting in the case of colloidal gels, to test this idea. This was done and the  $W_6$  distribution in a colloidal system undergoing gelation is shown in figure 9(a). The results were *extremely* disappointing, with hardly any change in the  $W_6$  distribution upon gelation [85].

Now colloidal gels, as figures 2(a) and 5(b) make plain, are not homogenous materials like liquids, rather they are highly inhomogeneous. Moreover the AO interaction between the colloids is rather different to the Lennard-Jones interaction (figure 5(a)). Notably it exhibits a hard core, and hard spheres and ‘sticky spheres’ have a distinct and more complex energy landscape than does the longer-ranged Lennard-Jones interaction [170–173]. Indeed it turns out that only in the limit of infinite interaction range, i.e. infinitely large polymers, does the icosahedron acquire the same binding energy as the crystal structures, suggesting that Frank’s hypothesis might not apply to colloid–polymer mixtures at all. This is due to the hard core in the AO model, and packing of spheres in an icosahedron requires either a small compression of the inner sphere or that the outer spheres do not touch one another, see figures 9(b) and (c).

Doye *et al* explored the effect of the interaction range on the minimum energy clusters [174], by considering the variable-ranged Morse potential (equation (17)). The Morse potential is controlled by its range parameter,  $\rho_0$ , and for  $\rho_0 = 6$ , it is rather similar to the Lennard-Jones interaction, and indeed the minimum energy cluster for  $m = 13$  particles is indeed the icosahedron. However, as shown in figure 5(a), for a range parameter

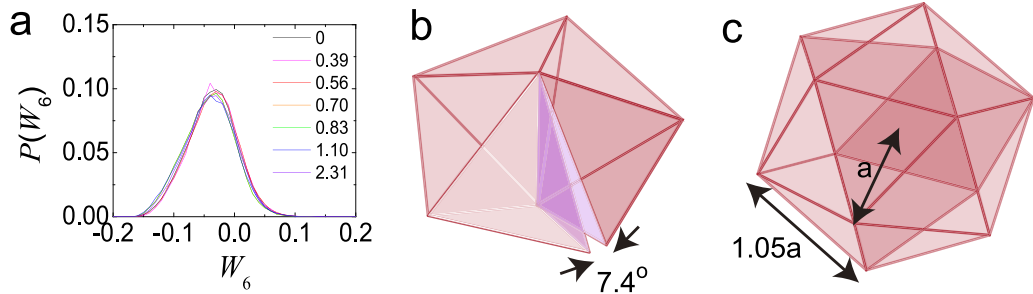


**Figure 9.** Geometric frustration in fivefold symmetric polyhedra. (a)  $W_6$  bond-order parameter distribution. Colours correspond to polymer weight fractions  $\times 10^{-4}$ . Here gelation occurred at  $c_{PG} = 7.7 \pm 0.7 \times 10^{-5}$ . Reprinted by permission from Springer Nature Customer Service Centre GmbH: [Springer Nature] [Nature Materials] [85] (2008). (b) The pentagonal bipyramid is constructed with five tetrahedra which leads to a gap of  $7.4^\circ$ . (c) 13-membered icosahedron. Icosahedra have bonds between particles in the shell stretched by 5% with respect to the bonds between the central particle and the shell particles. Reprinted from [70], Copyright (2015), with permission from Elsevier.

$\rho_0 = 33$ , the interaction is very similar to an AO interaction for a polymer–colloid size ratio  $q = 0.18$  and in this case, the icosahedron is not the minimum energy structure.

There is further consideration which suggests that minimum energy clusters may be appropriate when considering the local structure of colloidal gels. Loosely speaking, clusters may be thought of as ‘zero-dimensional’ objects. Bulk liquids, of course, are three-dimensional. What this means is that while, for example the icosahedron is the minimum energy cluster of 13 particles in isolation, this is not *a priori* valid in a bulk liquid. In fact, taking a mean-field treatment of the surrounding liquid, Mossa and Tarjus showed that indeed the icosahedron is still the minimum energy structure in a bulk Lennard-Jones liquid, albeit with a significantly reduced energy benefit with respect to other structures, compared to 13 particles in isolation [175]. More troubling is the observation that in the Lennard-Jones liquid at the triple point, only one particle in a thousand is part of an icosahedron [176], although upon supercooling (in the absence of crystallisation) the population increases markedly in a variety of systems [89, 94, 177–179]. Consideration of colloidal gels, as shown in figures 5(b) and 6(b), suggests that in thinking of the ‘arms’ of the gel to be quasi-one dimensional, we may expect that the clusters might be a reasonable description of the local structure of a colloidal gel.

The idea of Frank, of 13-particle icosahedra, could therefore be extended in two ways. Firstly, minimum energy clusters appropriate to colloid–polymer mixtures should be considered, and here we appeal to the work of Doye *et al* [174]. Secondly, given the inhomogenous nature of the material, we expect that cluster sizes other than  $m = 13$  would be appropriate. To address this, the *topological cluster classification* (TCC) was developed [85, 180, 181]. This algorithm detects groups of particles whose bond network is identical to the minimum energy clusters depicted in figure 10. The transition in cluster population from the ergodic fluid (dominated by particles not in a cluster, rendered in grey in figure 10) to the gel which is dominated by particles in clusters, such as the five-membered triangular bipyramid rendered in white and five-fold symmetric eight-membered cluster rendered in red is dramatic, especially given the failure of the bond-orientational order parameter  $W_6$  (figure 9(a)).

The importance of clusters was later emphasised in work which related long-lived and stable clusters to the mechanical properties of gels, and also explored the role of isostaticity [182]. The role of isostaticity gained further traction in an ingenious series of experiments performed by Tsurusawa *et al* [183]. Here the process of gelation was observed *in situ*. The emergent rigidity of the gel network was identified with a strong increase in the population of six-fold coordinated (isostatic) particles, and in particular a network of these. Related ideas have been expressed recently, this time focussing on contacts between clusters [184]. And indeed, clusters have been postulated as a mechanism for gelation due to their packing [106]. Given that many of these papers use one or other method to analyse their data, it is hard to escape the impression that the different analyses are different facets of the same phenomenon: there is a clear motivation to apply a range of analysis techniques to a single set of data.

*Criticality.*—Spinodal gelation in sticky sphere-like systems with short-ranged attractions is intimately related to liquid–gas demixing (figure 2) [48]. One may enquire what happens around the critical point. Naively one imagines the fluid side is similar to a system with long-ranged interactions where liquid–gas demixing is thermodynamically stable. It is as if the system does not ‘know’ that it will undergo gelation upon crossing the phase boundary rather than demixing. Thus one can determine the correlation length  $\xi$  of density–density fluctuation approaching criticality. As shown in figure 11(a) it is consistent with the onset of critical scaling [165], which is known to apply rather far from criticality, indeed until  $\xi \approx \sigma/2$  [186]. On the gel side, the correlation length does not obey critical scaling, as the system is not in equilibrium. These density fluctuations lead to a substantial increase in the cluster population (figure 11(b)), though little evidence of crystalline clusters is found even close to criticality (which might have been expected from the increase in nucleation rate in the vicinity of the critical point see section 5.2).

## 5. Dynamical properties of colloidal gels

We have discussed above mechanisms for solidification in colloidal gels. We now turn our attention to dynamical behaviour.

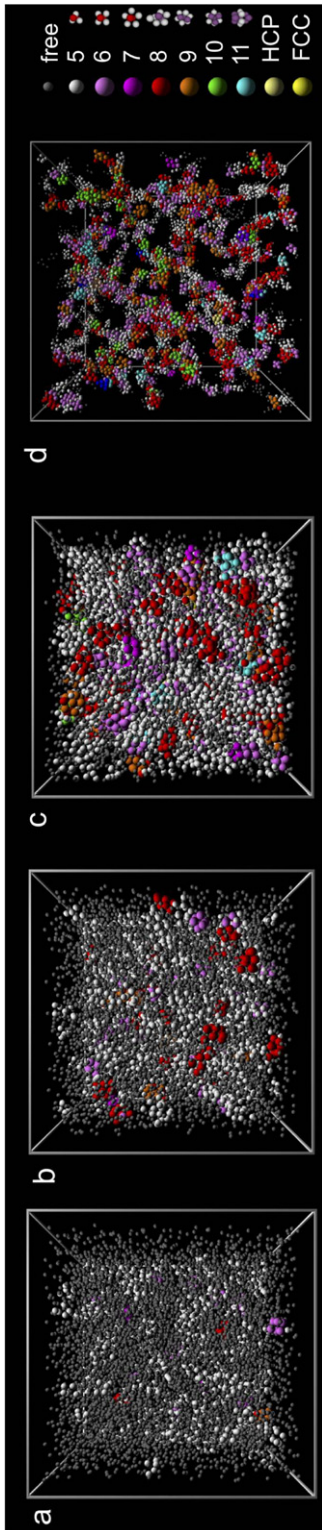


**Figure 10.** Coordinates identified as belonging to different clusters. (a) Colloidal fluid, polymer mass fraction  $c_p/c_{pg} = 0.73$ . (b) (Ergodic) liquid close to gelation,  $c_p/c_{pg} = 0.92$ . (c) Colloidal gel,  $c_p/c_{pg} = 1.4$ . (d) Dilute gel  $\phi = 0.05$ ,  $c_p/c_{pg} = 2.28$  showing percolating cluster structure. Particles are colour-coded according as follows: grey, free (not in any cluster) shown 0.4 actual size, white,  $m = 5$ , shown 0.6 actual size. Yellow, crystalline, shown 0.8 actual size. Other particles are members of cluster of size  $m$  given by the colours, shown 0.8 actual size. Here  $c_{pg}$  is the polymer concentration required for gelation. Reprinted by permission from Springer Nature Customer Service Centre GmbH: [Springer Nature] [Nature Materials] [85] (2008).

This can be interpreted at three levels, pertaining to different timescales:

- Timescales where the properties of the gel as a whole remain largely unchanged. In this regime, most results concern single-particle motion and the timescales are short, on the order of the Brownian time  $\tau_B$ .
- Timescales, over which there is significant ageing or even failure of the gel. Here the properties of the gel change measurably over time. Depending on the age of the gel, these can be short ( $\sim \tau_B$ ) or long ( $\gg \tau_B$ ).
- Timescales related to (periodic) deformation such as through shear or flow. In this instance the dynamical mechanisms at play are strongly related to the choice of deformation rate.

Before discussing each case, we emphasise that for particle-resolved studies, an important consideration is particle-tracking errors [43, 187]. In the case that particles move rather little, say  $\lesssim 0.1\sigma$ , it is likely that particle tracking errors can contribute significantly to the measured displacements, it is often hard to distinguish what is a ‘real’ movement and what emerges from the limitations of the tracking analysis, and this should be borne in mind when interpreting data.

### 5.1. Short-time dynamics

In the case of short-time dynamics, it is natural to consider dynamic heterogeneity. This has been extensively studied in supercooled liquids and glasses since its discovery by Harrowell and co-workers in the early 1990s [188]. In the case of glasses and supercooled liquids, which are rather homogenous, dynamic heterogeneity pertains to regions where the particles relax at different rates, but the structure is often rather similar between slow and fast regions [70].

Gels, with their inhomogeneous nature present many interfaces between the ‘arms’ of the gel and voids in between the arms and indeed here the particles have fewer neighbours and can move more easily [83–85, 161, 190]. Thus we expect that the most mobile particles may be located at these interfaces, and indeed the first study of dynamic heterogeneity in gels, using computer simulation, found precisely that [55]. Particle-resolved studies of dynamic heterogeneity in gels began with Gao and Kilfoil who found distinct populations of slow and fast particles [83]. Later work confirmed this [85, 86, 191, 192] as shown in figure 12(a). It is important to note that in this sense, dynamic heterogeneity in gels is profoundly different to that in the more homogenous supercooled liquids and glasses where there are no interfaces. Furthermore gels are far-from-equilibrium and the ageing is much more significant: supercooled liquids are typically metastable to crystallisation, but their properties are usually stable over many relaxation times, unlike the case of colloidal gels formed via spinodal decomposition. It is possible that, deep inside the ‘arms’ of a gel, there may be dynamic heterogeneity of a similar nature to that in supercooled liquids [188], but to our knowledge, no such investigation has been made.

Curiously, in the density-matched PMMA system (section 4.1), Solomon and co-workers found a peculiar kind of dynamic heterogeneity [84]. The observation was that

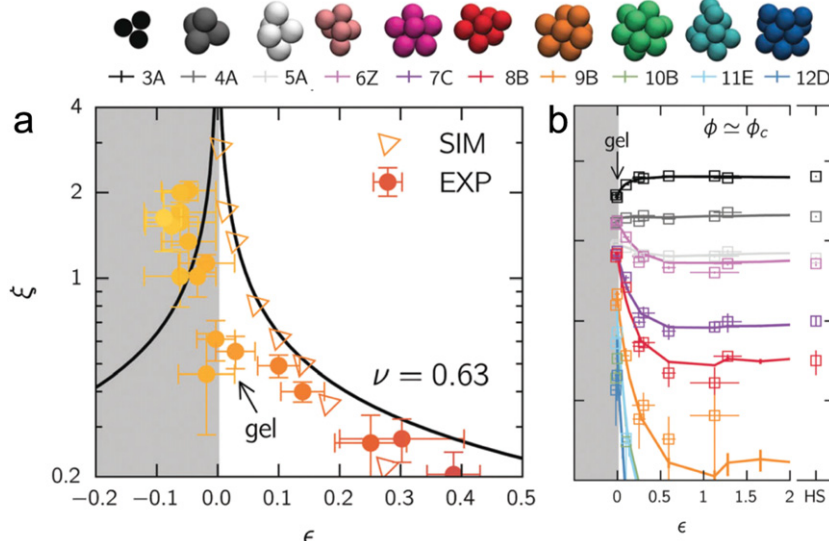


**Figure 11.** Critical behaviour in colloidal gels. (a) Correlation length of density–density fluctuations  $\xi$  as a function of the reduced effective temperature  $\epsilon = (c_p^c - c_p)/c_p$  for the volume fraction corresponding to the critical isochore  $\phi_c^c$ . (b) Population of TCC clusters (indicated above) as a function of the reduced effective temperature  $\epsilon$ . Reproduced from [185] with permission of The Royal Society of Chemistry.

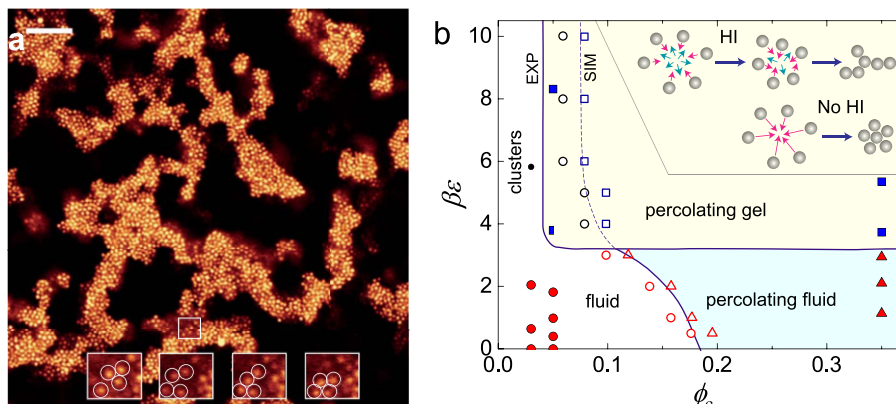


**Figure 12.** (a) Localised particle-hopping on the surface of an arrested gel network. Magnified snapshots of an area (small box) are shown in the four larger boxes as a time-sequence. The particles undergo a local re-arrangement over  $\sim 500$  s, as indicated by the outlined particles. The snapshots are taken at  $t_w = 320, 410, 420$  and  $460$  s after imaging began, which correspond to  $460, 590, 600$  and  $660\tau_B$  respectively. Here the polymer concentration with respect to that required for gelation  $c_p/c_p^g = 3.90$ , polymer–colloid size ratio  $q = 0.49$ , and volume fraction  $\phi = 0.2$ . Scale bar in top left-hand corner indicates  $10 \mu\text{m}$ . Reproduced from [86] with permission of The Royal Society of Chemistry. (b) State diagram showing gelation in an experimental and simulated system in the  $\beta\epsilon$  (potential well depth)- $\phi$  (colloid volume fraction) plane with  $q = 0.18$ . Phase separation is observed for  $\beta\epsilon \gtrsim 3$ . Filled symbols are experimental data, Brownian dynamics simulation data are unfilled symbols. Red symbols are one-phase fluids, circles lie below the percolation threshold, triangles above. The main result here is that the experiments (with hydrodynamic interactions) percolated at much lower volume fraction than the Brownian dynamics simulations (without long-ranged hydrodynamics). Black circles are (non-percolating) cluster fluids. Blue squares are gels. Inset shows effects of hydrodynamics on colloidal aggregation. Top line: hydrodynamic interactions lead to solvent flow (cyan arrows) which influences the motion of the aggregating colloids. The incompressibility of the fluid allows only transverse (rotational) flow, resulting in the formation of an elongated structure rather than a closed one. Bottom line: no hydrodynamic interactions. Their attractive interactions lead the colloids to aggregate (pink arrows) to form a compact structure. Reprinted (figure) with permission from [189], Copyright (2015) by the American Physical Society.

the mobility depended on the number of neighbours that a particle had in a weakly quenched gel (with a small amount of polymer) and not in the case that more polymer was added such that the gel could be regarded as more deeply quenched. In the former case, the gel had a cluster-like structure while the latter case the structure was described as ‘stringlike’. It is worth noting that this was inferred from 2D measurement of the dynamics, and revisiting this phenomenon with 3D

tracking and/or computer simulation (subject to the discussion above in section 4.1 and reference [138]) would be interesting. Some work has been carried out in this direction: in a study with a solvent of dielectric constant  $\sim 2$  so that electrostatics were very weak, Ohtsuka *et al* [161] found that close to gelation, the colloidal fluid exhibits transient but rather long-lived clusters where again mobility depended on the number of neighbours.

### 5.2. Evolution: aggregation, ageing and crystallisation

Ageing of quiescent (unperturbed) colloidal gels has been studied on two timescales. Short timescales ( $\sim \tau_B$ ), *prior to arrest* under which the gel assembles and follows spinodal decomposition and long timescales ( $\gg \tau_B$ ) of post-arrest coarsening. A major effect on the former, short timescale case, is the role of hydrodynamic interactions induced by the solvent. This effect was first emphasised by Furukawa and Tanaka using computer simulation with the hydrodynamics included [193]. It was later shown that including hydrodynamics in simulation gives a much more accurate reproduction of the experimental formation of gels than does Brownian dynamics simulations, which do not consider the effect of hydrodynamic interactions between particles [189]. The principle effect appears to be that the outflow of solvent in condensing clusters of colloids in the very initial stage when density inhomogeneities emerge leads to much ‘stringier’ clusters of colloids than those found in Brownian dynamics simulations, though nevertheless the particles in the experiments have been found to be isostatic [194]. As shown in figure 12(b), these then percolate at a volume fraction *a factor of two* less than is the case for Brownian dynamics simulations under the same conditions. It is important to note, however, that any link between volume fraction and percolation must have a timescale associated with it. This is because the clusters formed by aggregating colloids have a fractal dimension less than three (typically 1.8–2) so that in the limit of long timescales of aggregation, the volume fraction required for percolation vanishes. This was first emphasised by Weitz and co-workers [195] and later demonstrated with computer simulation [80]. Very recently, novel particle-resolved experiments where the cluster aggregation could be initiated *in-situ* have been carried out (which are similar in spirit to reference [196] in section 4.3). The cluster size as a function of time can be followed directly, as shown in figure 13. This has been made possible by the use of critical Casimir forces [39, 40].

At longer timescales, where dynamical arrest of the colloid-rich phase occurs, ageing, the irreversible change of the properties of the gel is a significant feature. This is essentially due to the fact that the colloid dynamics is not totally arrested, it is rather *slowed*. Moreover, relative to the homogeneous supercooled liquid the interfaces in the gels mean that there is another mechanism of relaxation. Thus on long timescales the gel network will exhibit the coarsening dictated by the spinodal decomposition (section 2.1). Such a scenario is shown in figure 14(a), an early 3D analysis of a very dilute (volume fraction  $\sim 0.01$ ) gel of 50 nm polystyrene particles formed through van der Waals attractions. It is possible that the strong van der Waals interactions in this system acted to suppress creaming (sedimentation where gravity ‘points in an unusual direction’) due to the polystyrene particles being lighter than the water solvent [197].

Another means to investigate the coarsening dynamics is to controllably accelerate the time-evolution of the system. Such an approach was used by Zhang *et al* [86] who reduced the volume fraction of the colloid-rich phase such that the dynamics accelerated (recall figure 4(a)). Zhang *et al* were thus able to

observe coarsening prior to sedimentation even in non-density matched depletion gels. This reduction in volume fraction was achieved in two ways. Firstly, a larger polymer–colloid size ratio  $q$  means that, for a given degree of effective ‘cooling’ with respect to the critical point, by adding more polymer, corresponds to a colloidal liquid of lower volume fraction [24]. That is to say, if one adds (say) 10% more polymer than that corresponding to criticality, the volume fraction of the colloid-rich phase is lower in the case of larger size ratio  $q$ . Secondly, if one reduces the concentration of polymer (approaching criticality), the volume fraction of the colloidal liquid decreases and, in principle, even very short-ranged effective attractions can result in colloidal liquids without arrest [199].

The local structural analysis underlying the process by which gels become rigid (section 4.3 and e.g. figure 10) can also be used to probe the change in local structure during ageing. It is seen here in figure 15 that for the system studied (with 8% polydispersity to suppress crystallization), ageing is consistent with an increase in local fivefold symmetry, via in the increase in population of the 10-membered defective icosahedron. This structure also happens to be the locally favoured structure in hard spheres upon supercooling [89, 94, 177]. In figure 15(a) we also see strong evidence for stiffening in the form of the increase in the structural relaxation time.

A further key aspect of ageing is crystallisation. For suitably monodisperse systems, gels are metastable to colloidal fluid-crystal phase coexistence [24], as shown in the early work on particle resolved studies of crystallisation in colloid–polymer mixtures by de Hoog *et al* [131]. Simulations found that a slow increase in attraction strength gave a higher degree of crystallinity in monodisperse systems interacting via the Morse potential (equation (17)). In a system with just 4% polydispersity system the effect was similar, although the degree of crystallisation was rather reduced [200]. Even highly polydisperse systems have been predicted to fractionate and crystallise for hard spheres [201] and there seems little reason to suppose that the same mechanism would not apply here. Around criticality, fluctuations have been shown to accelerate crystallisation [202] and this has been reproduced in real space analysis of colloid–polymer mixtures [203, 204]. Alternatively, crystallisation can occur in the ‘arms’ of the gels, as shown in figure 14(b) [198]. Interestingly it has been shown that this is an unexpected example of the Bergeron process which underlies atmospheric ice crystallisation, where particles ‘evaporate’ from the amorphous arms of the gel and then condense onto a crystalline region [196].

### 5.3. Failure: collapse under gravity

A particularly intriguing and challenging problem in colloidal gels is collapse under gravity [53, 205–207]. While we have noted above in section 4.1 that considerable efforts have been made to density match colloids and solvent to mitigate the effects of gravity, firstly, perfect density matching does not exist, secondly and more importantly, colloidal gelation is exploited to suppress sedimentation in a wide range of products such as coatings, crop protection suspension formulations, pharmaceutical suspension formulations, various cosmetic

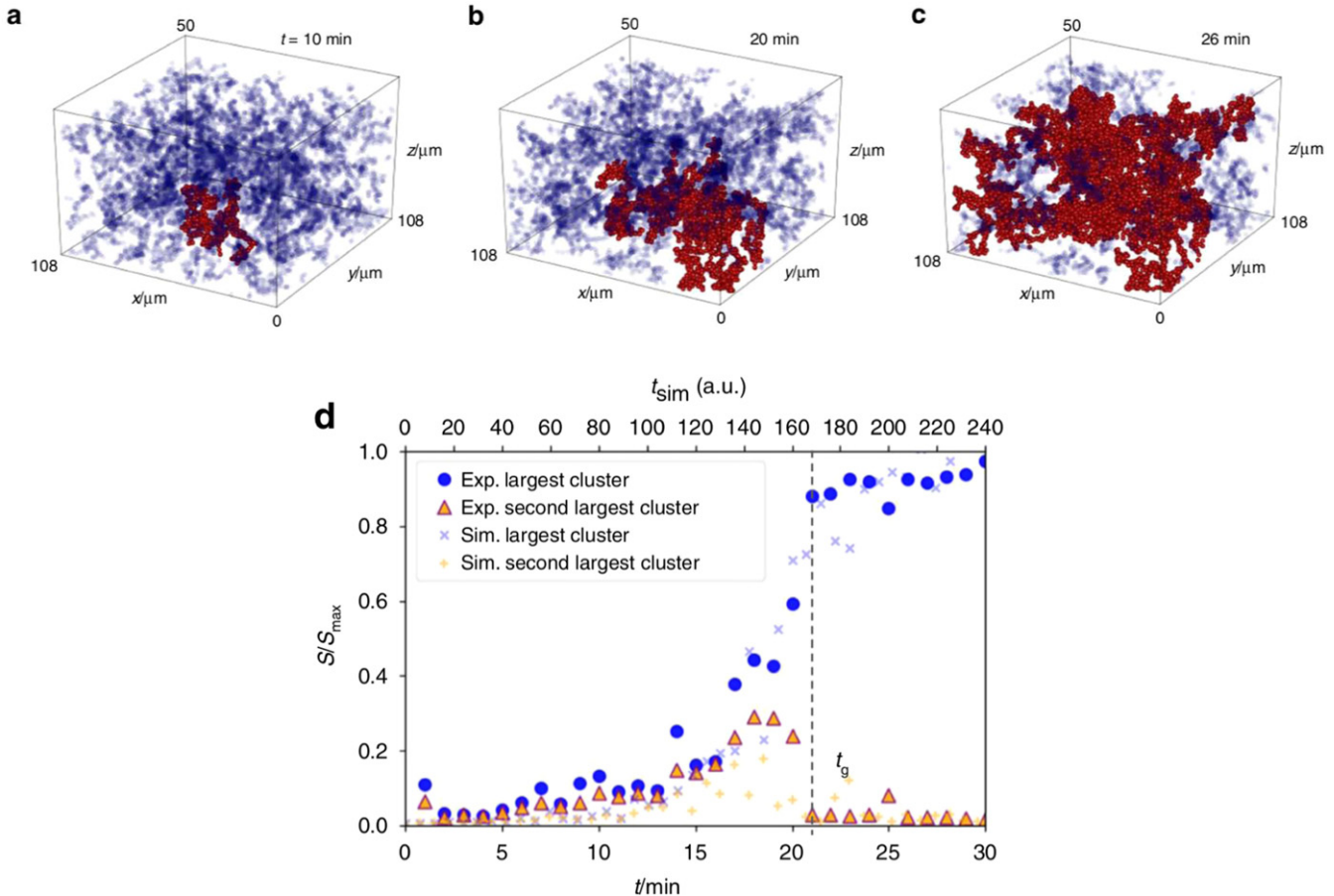


**Figure 13.** Experimental and computer simulation observation of aggregating colloidal particles interacting with critical Casimir forces at the times noted. (a)–(c) Largest connected cluster is marked in red. (d) Size of the largest, and second-largest cluster normalized by the maximum cluster size as a function of time. Reproduced from [39]. CC BY 4.0.

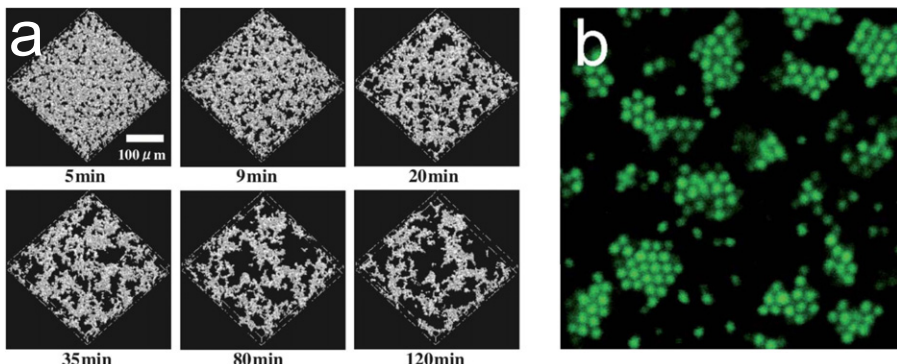


**Figure 14.** (a) Temporal change in 3D phase-separation patterns ( $240 \mu\text{m} \times 240 \mu\text{m} \times 80 \mu\text{m}$ ) during phase separation. The system was 50 nm diameter polystyrene particles in water. Reproduced from [197]. © IOP Publishing Ltd. All rights reserved (b) Crystallisation in the ‘arms’ of a colloidal gel with  $u_{AO} \approx 5.5k_B T$  and  $\phi_c = 0.12$ . Reproduced from [198] with permission of The Royal Society of Chemistry.

formulations, pigment printing inks, dispersions for 3D printing, ceramic preparations, food preparations, detergent formulations and home care products among many others for example. In equilibrium, or at least, in well-aged systems, many intriguing phenomena of hard and sticky spheres have been explored in the elegant work of Piazza and co-workers, who have largely focussed on rather smaller colloids than are amenable to real space imaging. From this and related work,

at least equilibrium sedimentation is quite well understood [208, 209].

Collapse falls into two categories. *Rapid collapse*, in which the system starts to collapse as soon as it is prepared [210] and *delayed collapse* in which little happens to the height of the top of the gel for some considerable time until, rather suddenly, it fails catastrophically and collapses in a timescale much shorter than the waiting time [62, 205]. Intriguingly, rheological work

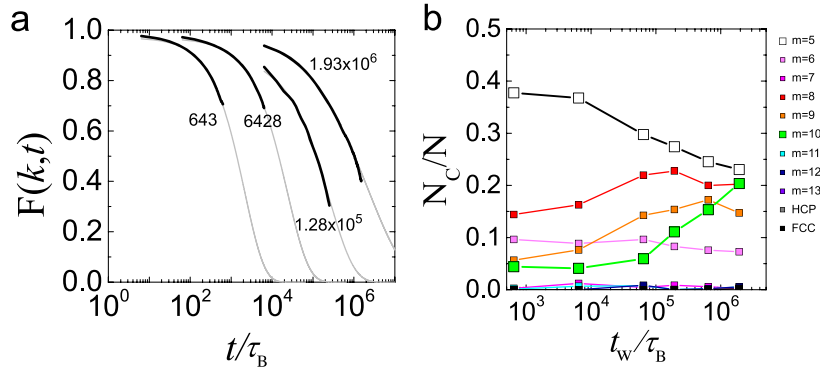


**Figure 15.** Stiffening (increase of relaxation time) and change in local structure in ageing gels. (a) Intermediate scattering functions from simulation data for a square well with range  $0.03\sigma$ , volume fraction  $\phi_e = 0.35$  and  $c_p/c_p^{\text{gel}} = 1.864$ . Different waiting times are expressed in units of the Brownian time  $\tau_B$ . Here the results from simulation (black lines) are fitted with a stretched exponential (grey lines). (b) Topological cluster classification analysis (see section 4.3 [180]) of the structural evolution as a function of waiting time  $t_w$ . TCC structures are illustrated in the legend right. Reprinted from [48], with the permission of AIP Publishing.

does suggest a coupling between collapse times, interaction strength and mechanical properties [211]. Overall, however, gel collapse is a poorly understood phenomenon, combining as it does highly non-equilibrium behaviour and two very distinct time-evolutions. It has been observed that often, larger systems (say  $>1$  cm in sample height) tend to exhibit delayed collapse while smaller systems can undergo rapid collapse. Some of us looked at the behaviour of a small system undergoing rapid collapse, see figure 16 [210]. Notably, these small, rapidly collapsing systems can be captured with particle-level computer simulation. It is worth noting that in the small system sizes as studied by Razali *et al* [210], even a drop of a few microns is readily measured, which would likely go unnoticed in larger systems. Moreover, in these small systems, the gravitational length of the colloids may be comparable to the system size. In this way, a hard sphere system would not sediment, but, as we see in figure 16, a gelling system does. This shows that, the interplay between gelation and sedimentation is *qualitatively* different between large and small systems. For now, the longer timescales and larger system sizes pertaining to delayed collapse remain beyond the grasp of direct particle-level simulation.

An example of the combination of real space analysis and rheology and direct observation is shown in figure 17. Here we see that little happens to the height of the gel  $h(t_w)$  but the storage and loss shear moduli both show an increase as a function of waiting time. In other words, the gel becomes *stronger* as it ages prior to catastrophic collapse, here after around  $10^5$  s storage and loss shear moduli both show an increase as a function of waiting time [63]. Here real-space analysis reveals coarsening of the gel prior to collapse, concurrent with a significant increase in the storage modulus, indicating that the gel is becoming stiffer.

#### 5.4. Bridging the gap between model systems and real world products

In the real world, the particles comprising colloidal gels are often no longer monodisperse or even spherical, sample sizes can be significantly larger (e.g. 0.1 to 10 L). Gels

have greater strength, stability timescales are much longer, secondary network ageing effects can occur such as Ostwald ripening (droplet/crystal growth) of colloidal emulsion droplets or suspensions of crystalline organic compounds such as active ingredients, many products are water based and importantly nearly all are opaque. Polydisperse silicone oil emulsions index matched in water/glycol/glycerol mixtures gelled with non-adsorbing polymers (hydroxyethyl cellulose, xanthan) which are more representative of real products have been developed and studies exploring how ageing of the network structure influences the rheology and gravitational stability in larger sample sizes [25, 63, 86, 212].

Interestingly such systems can reproduce features of both academic and industrial systems allowing academic research to be applied to real-world challenges with a key finding coming from *in-situ* vane rheology measurements in relatively large samples (height  $\approx 4$  cm) that the gel strength increases during ageing until collapse occurs, rather than collapse occurring because the network is becoming weaker, and therefore that the gravitational stress within the sample must also be increasing until it exceeds the strength of the gel (see figure 17) [25, 63]. Such systems are invaluable in exploring the larger scale ageing and gravitational stability of colloidal gels since they can be readily prepared in large volumes (5–10 L) and help to answer the pressing challenges of colloidal gelation. Another interesting feature of polydisperse systems is that they do not form colloidal crystals on experimental timescales, allowing ageing to be studied in shallow quenches closer to the spinodal line.

#### 5.5. Deformation

In many real world applications of gels, they undergo deformation as they are squeezed or scraped out of their containers. Therefore it is pertinent to ask how these materials change when they are sheared or when they flow. While solids respond elastically and liquids flow in response to deformation, complex fluids such as gels can show a combination of both responses: they respond elastically below a critical strain or stress, while beyond a characteristic yield strain or stress they

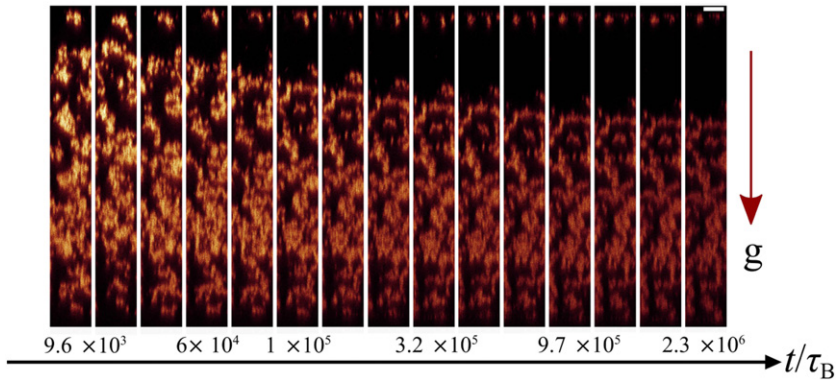


**Figure 16.** Time-sequence of sedimenting gels captured from a PMMA system in *cis*-decalin with a contact potential of around  $7.0k_BT$ . The scale bar in corresponds to  $7.5\ \mu\text{m}$ , the system is around  $100\ \mu\text{m}$  in height. Reproduced from [210] with permission of The Royal Society of Chemistry.

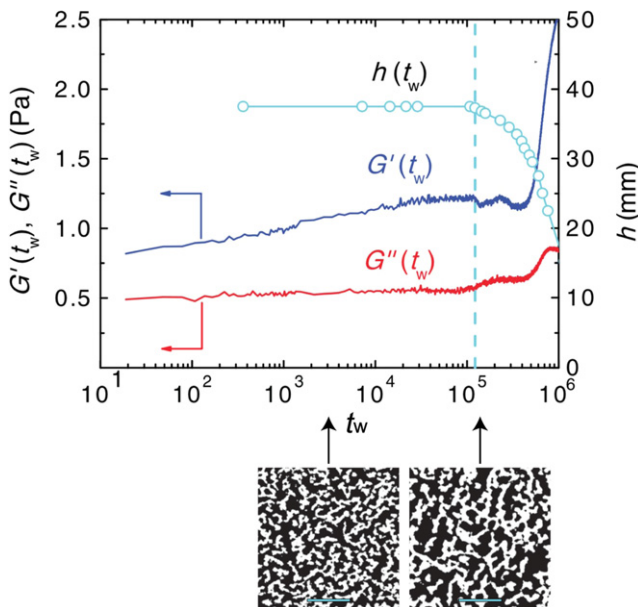


**Figure 17.** Combining techniques to investigate delayed collapse. Direct observation reveals the macroscopic height of the sample  $h(t_w)$ . Storage and loss moduli determined from rheology show a change in the mechanical properties, particularly the storage modulus  $G'(t_w)$ . This indicates an increase in stiffness of the material over time. Binarised confocal images (bars =  $40\ \mu\text{m}$ ) show the time-evolution of the structure. Reprinted (figure) with permission from [63], Copyright (2012) by the American Physical Society.

flow [111, 112]. Typically the response to shear is measured using rheometry, which yields the elastic (storage)  $G'$  and viscous (loss)  $G''$  moduli. The transition between liquidlike and solidlike response, such as by progressively increasing polymer concentration to increase the attraction strength between colloidal particles, is evidenced by a crossover between  $G'$  and  $G''$  at lower frequency, while for a gel  $G'$  is greater than  $G''$  in the elastic regime. One measure of yielding is, at large strains ( $\gamma \geq 10\%$ ),  $G' < G''$ . For a gel however, the decay of  $G'$  and  $G''$  with increasing strain provides evidence of residual structure until  $\gamma > 100\%$  [108, 213]. Indeed, Hsiao *et al* [182] note that for a comparable system of non-interacting particles,  $G'$  is too small to measure for ( $\gamma \geq 15\%$ ), yet for a seemingly fluidised gel sample, there is still some contribution to

rigidity for strains of at least 60%. Through simultaneous confocal imaging during shear, they attribute this to hydrodynamic coupling between a sub-population of stress-bearing, rigid particle clusters which imparts some rigidity to the gel—despite breakdown of the quiescent percolating gel network.

When studying the flow or shear of colloidal gels it is useful to consider the Péclet number,  $\text{Pe} = \dot{\gamma}\tau_B$ , where  $\dot{\gamma}$  is the shear rate and  $\tau_B$  is the Brownian time. For a gel, large Péclet numbers correspond to a simple viscous response (stress increasing linearly with shear rate), as the gel structure is rapidly broken up, while small Péclet numbers result in a soft-solid response (displaying a yield stress plateau).

While the rheological response of gels provides compelling evidence of their time-dependent structure, it is useful to *simultaneously* image gels under shear to directly relate mechanical information to changes in gel configuration. To perform real-space imaging and shear measurements simultaneously, one of two approaches are typically used: a confocal optical setup is used with a (modified) conventional rheometer [214], or a custom shear stage is used that can be mounted directly to a commercial confocal microscope [130, 215, 216]. Similarly, measurements under applied flow typically use a custom flow cell with a standard microscope [217, 218].

**5.5.1. Shear.** As with a polymer gel, shear can act to coarsen or melt the gel structure. Further (detectable) complexity is also accessible in the formation of locally favoured and/or crystalline structures. Smith *et al* [215] used a custom parallel plate shear cell where both plates were moved in opposite directions, accessing a stationary plane in the centre of the sample (as opposed to a stage with a single mobile plate, for which the stationary plane is the fixed plate) to shear a very stiff ( $u_{AO}/k_BT = -46 \pm 16$ ) colloid–polymer mixture (PMMA-polystyrene in a density and refractive index matching solvent mixture, section 4.1). They found that gel yielding and crystallisation occur concurrently, and that the strain required increased with decreasing shear frequency, while for high strain values the crystallites were melted. Figure 18 shows the rich variety of shear-induced structure for a typical sample, including small crystalline, large crystalline domains and large voids.

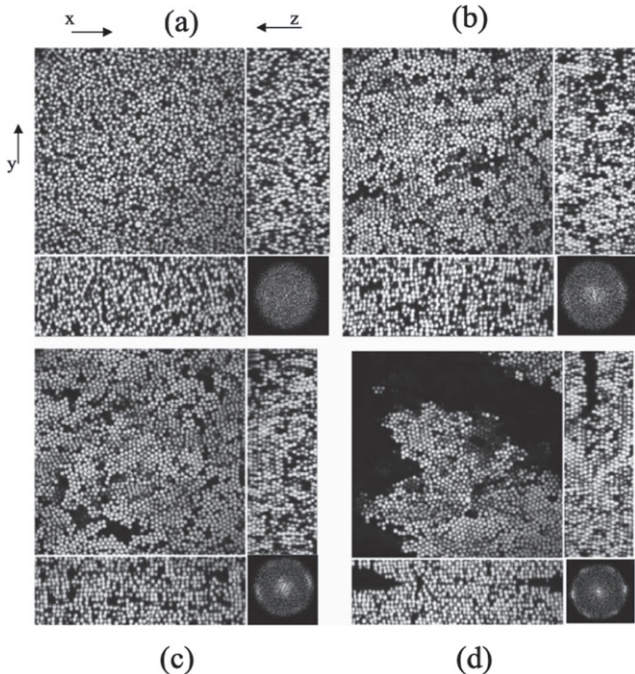


**Figure 18.** Confocal microscopy images of a colloid–polymer gel ( $\phi = 0.4$ ) after 31 min of oscillatory shear at a frequency of 70 Hz and a strain amplitude of 0.15. (a) Shows the gel in its quiescent state. (b)–(d) Shows typical, highly ordered and void-rich regions respectively. All regions are shown in  $xy$ ,  $xz$  and  $yz$  slices and a representative fast Fourier transform is also shown. Reprinted (figure) with permission from [215], Copyright (2007) by the American Physical Society.

Koumakis *et al* [214] also applied shear to a colloid polymer gel of similar composition to Smith *et al* [215] (albeit with slightly less strong attractions of  $-16k_B T$  and  $-23.2k_B T$ ). Utilising a modified rheometer to apply shear to the gel, imaged *in situ* with a confocal insert, it was possible to study the interplay between microstructure and mechanical properties. Gel microstructure was characterised through the void distribution and the average number of interparticle bonds. For high shear rates complete cluster melting was observed, while for smaller rates cluster compactification occurred, producing significant structural inhomogeneity. By studying the time evolution of gels prepared with high and low pre-shear, it was shown that strong pre-shear resulted in homogeneous, stronger solids (analogous to an instantaneous thermal quench), while weak preshear lead to heterogeneous weaker gels (analogous to low rate thermal quenching, resulting in the formation of more compact clusters than possible by Brownian relaxation alone). Unusual void formation was also reported by Kohl and Schmiedeberg [219] in Brownian dynamics simulations of shear flow of relatively soft gels ( $u_{AO}$  between  $-2.2k_B T$  and  $-6.1k_B T$ ). Rather than randomly distributed, isotropically oriented domains reported previously, they discovered ‘slab-like’ domains in sheared gels that emerged over many shear cycles (figure 19). This behaviour persisted to high shear strengths before eventually being shear melted. This unusual structure was compared to the syneresis phenomena that are observed in a variety of gelling systems.

The ability to encode structural or mechanical properties into a gel through specific shear conditions as a form of ‘memory’ was recently explored by Schwen *et al* [220] using a custom biaxial shear stage [216] on a confocal microscope. By using many shear cycles at a given strain to ‘train’ the gel, strain memories were embedded, such that a reversible structural rearrangement (where the image difference before and after strain was small) in response to further strains *below* the training strain amplitude was observed: in effect, a new yield strain is set for the gel at the training strain. However for large strains this was not the case—the applied strain would always result in rearrangements. Remarkably the memory was also encoded orthogonally to the shear direction: that is, shear applied along the  $x$ – $z$  shear plane also resulted in a new yield strain along the  $x$ – $y$  shear plane. The main structural transformation during this process appeared to be an increase in mean contact number for the trained gel. Indeed, particles most likely to move between shear cycles were those with fewer number of contacts.

*Shear banding*, a commonly observed feature in colloidal glasses and yield stress fluids [112] has been observed using magnetic resonance imaging for a colloidal gel [221]. This real space technique, with less resolution than microscopy, but not requiring special preparation of the material such as (refractive index matching) serves as a useful complement to confocal microscopy. It is also possible to study shear banding using the set-up noted above, combining a confocal microscope and a rheometer [222]. Bonn and co-workers demonstrated the role of using rods as a bridging mechanism between emulsion droplets to cause gelation and were able to relate the rheological behaviour of thixotropic and so-called simple yield stress fluids [222]. Shear banding is intimately related to so-called viscosity bifurcating fluids, where for certain stresses the material can catastrophically fail, with a massive drop in its viscosity [111, 112]. A predominantly rheological study which incorporated some real space imaging by Sprakel *et al* showed intriguing scaling of the increase in strength of the gel prior to yielding which could be accounted for by a simple model [223].

**5.5.2. Flow.** The behaviour of colloidal gels flowing under narrow confinement is widely applicable to many real-world situations, such as in biological systems or soft robotics. In most shear measurements the shear is typically uniform, whereas a real-world system might combine nonuniform shear and hydrodynamic forces as the fluid experiences different levels of constriction, such as in a dispensing nozzle. Various experiments and simulations have attempted to address these differences.

Han *et al* [224] used hydrodynamic simulations to explore the behaviour of a colloidal gel subject to microchannel flow. High shear flow acts to disrupt any clustering, while for low shear flow the colloids form gel like clusters and small crystal nuclei. For intermediate shear flows (where the global shear forces approach the same magnitude as the attractive forces between the particles) crystallisation is greatly enhanced. In the regime between crystallisation and melting the

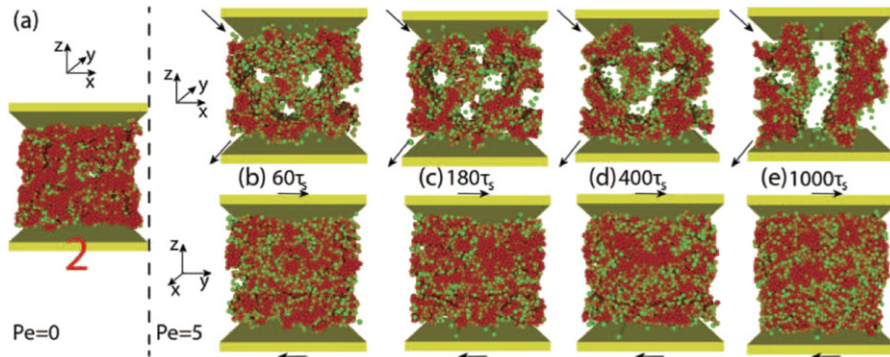


**Figure 19.** Brownian dynamics snapshots of gel ( $U_{AO} = 4.4k_B T$ ) over many shear cycles (indicated (b)–(e)) compared to quiescent case (a). While the  $yz$  projection shows little change in structure or bond number (where red indicates 5 or more bonds, green 1 or fewer), the  $xz$  plane (perpendicular to the shear direction) shows the emergence of pronounced gel-slabs held between the upper and lower plates, separated by voids. Reprinted by permission from Springer Nature Customer Service Centre GmbH: [Springer Nature] [The European Physical Journal E – Soft Matter] [219] (2017).

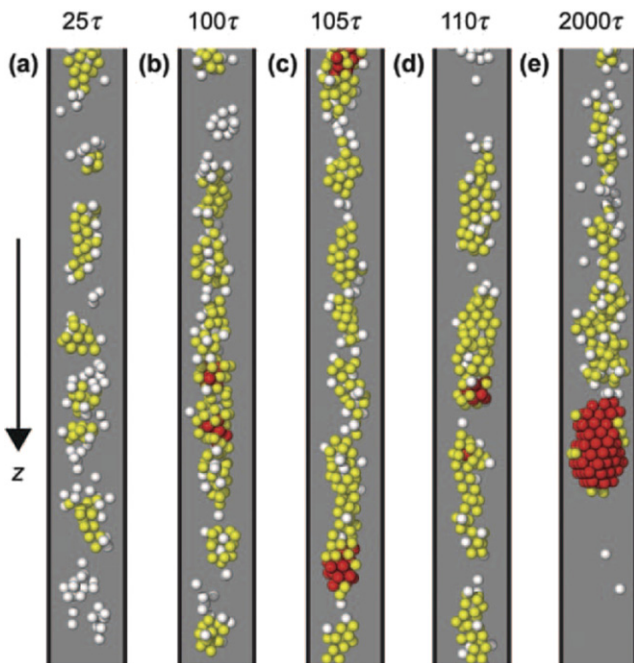


**Figure 20.** Time dependence of cluster structure in microchannel flow. (a) Shear flow acts to align attractive clusters along channel axis that form connected strands (b). Threads form series of ‘packets’ (c) before breaking up into crystalline droplets (d), which become increasingly ordered over many cycles (e). Colour coding indicates colloidal gas (white), liquid (yellow) and crystal (red). Reproduced from [224] with permission of The Royal Society of Chemistry.

non-uniform shear results in crystalline cluster cores localised in the channel centre, but melting at the cluster surfaces. This effect was reduced for wider channels as the flow becomes more uniform. Remarkably they also noted gel-strand formation along the channel axis, that repeatedly break up into increasingly crystalline droplets. This is shown in figure 20 for average shear forces 1.4 times attractive forces.

Conrad and Lewis used confocal microscopy to study the flow of a silica-polyelectrolyte colloidal gel in a microchannel of width  $\sim 50$  diameters [225]. High flow rates prevented 3D imaging during measurements (owing to the slow framerate

of recording a 3D stack). As with the simulations, they note that the network structure of a quiescent gel is disrupted during shear flow, first into small clusters, then smaller clusters and individual particles with increasing pressure. They also note a transition from pluglike to fluidlike flow beyond a critical shear rate. They also used a similar setup to study the structure of a colloidal gel passing through a channel constriction [226], and found evidence of filter pressing as the particle concentration increased in the constriction. They also noted failure of the gel network at cluster boundaries. For small shear pluglike flow was observed, but as for the straight channel, at high shear the flow became fluid-like. They also found that a stagnation zone developed close to the constriction, resulting in transient wall jamming and further disruption of the gel network, leading to fluidization further downstream.

## 6. Introducing complexity: anisotropy and mixtures

Gels can be formed from systems other than spherical colloids with an (effective) attraction. Complexity may be introduced via anisotropic particles such as rods and platelets. Depletion gels formed of colloidal rods may form at very low volume fractions for suitably high aspect ratio rods and have been reviewed by Solomon and Spicer, who suggested that the structures assumed by the rods could be interpreted as ranging from fractal clusters to homogeneous rod networks [227]. An important observation in the case of gels formed of rods is that percolation can occur at very low volume fraction, with implications for materials based on percolation such as photovoltaic cells (which rely on percolation of conducting particles) [228, 229]. It is important to note that the equilibrium phase diagrams of rods interacting through depletion interactions are rather more complex than those of spheres, due in no small part to the emergence of a number of liquid crystalline phases [230] and thus one may expect complex mechanisms of gelation. Real space analysis of rods took a step forward with the development of polyamide rods in the group of Solomon, which revealed a novel bundling transition, as shown in figures 21(a) and (b). The same group managed to form discoids, by compressing

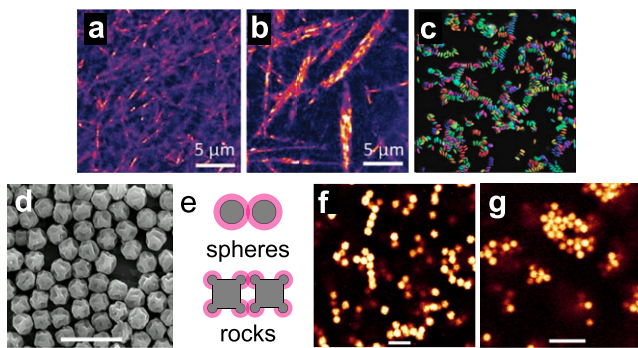


**Figure 21.** Depletion-induced gelation in anisotropic colloids. (a) and (b) Bundling in colloidal rods. (a) Confocal image showing a mobile rod network with no added polymer. (b) Bundled structures for a rod suspension with  $c_p/c_p^* = 0.52$ . Reprinted with permission from [232]. Copyright (2009) American Chemical Society. (c) Chain-like clusters of PMMA discoids. Reproduced from [231]. CC BY 4.0. (d) SEM image of colloidal ‘rocks’. (e) Schematic showing the mechanism of rigid bonding in the rocks contrasted with spheres. (f) Confocal microscopy image of a gel of rocks  $c_p/c_p^{\text{gel}} = 1.13$ . (g) Confocal microscopy image of a gel of spheres  $c_p/c_p^{\text{gel}} = 1.44$  scale bars in (d), (f) and (g) are  $10 \mu\text{m}$ . Reproduced from [233] with permission of The Royal Society of Chemistry.

PMMA above its glass transition temperature and then redispersing it. The resulting discoids formed chains with their flatter sides oriented towards one another, which would maximise the overlap volume and thus be favoured by the depletion interaction (figure 21(c)) [231].

Another form of anisotropy was explored by Rice *et al* [233]. As shown in figures 21(d)–(g), here colloidal ‘rocks’ assembled into gels. Notably, the rocks developed highly rigid bonds between the particles, as it was hard for the rocks to roll around one another compared to spheres (figure 21(d)).<sup>10</sup> These rigid bonds led to rather linear chains one particle thick, markedly different from the more compact clusters formed of spheres and in fact reminiscent of the ‘empty liquids’ mentioned in section 4.2 [21].

A further means to increase the complexity of the system is to introduce further species. This was done by Zhang and co-workers, where binary colloids and polymer were investigated, as shown in figure 22 [234]. The size ratios were approximately 4:2:1 for the large colloids, small colloids and polymer, respectively. A superficial analysis of equation (16) might suggest that, upon increasing the polymer concentration, the larger colloids would start to demix prior to the smaller particles as the big–big depletion interaction is much stronger than the small–small depletion interaction, as indicated in figure 22(a2). However, the reality is more intricate with a single critical point for the entire three-component system, which separates into two mixed phases (figure 22(a1)). Further addition of polymer results in a complex composition inversion phenomenon, where upon demixing the colloid-rich phase is initially dominated by the larger colloids but this effect lessens dramatically as further polymer is added, ultimately resulting in arrest of the colloid-rich phase and gelation [234].

<sup>10</sup> The case of very small polymers which lead to stabiliser interdigitation notwithstanding, see section 4.1 [145].

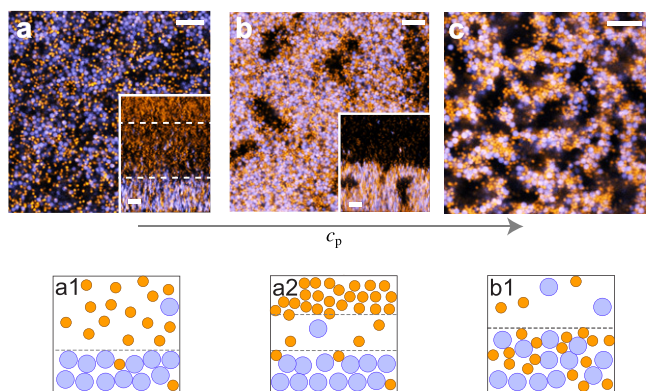


**Figure 22.** Phase behaviour of binary colloid–polymer mixtures. (a)–(c) Confocal microscopy images (see text) with larger colloids (blue) and small (orange). Insets show  $xz$  profiles which are  $100 \mu\text{m}$  in height. (a)  $c_p/c_p^* = 0.059$ ; possible two- or three-phase demixing as indicated by dashed lines in inset. (b)  $c_p/c_p^* = 0.069$ ; (c)  $c_p/c_p^* = 0.090$ , gelation. Scale bars denote  $10 \mu\text{m}$ . Possible scenarios by which the experimental data may be interpreted: (a1) two-phase coexistence—the lower (liquid) phase is rich in large particles and the upper (vapour) phase is rich in small particles and polymer; (a2) the colloidal mixture exhibits liquid–liquid demixing. (b1) Upon deeper quenching more small particles become entrained in the colloid-rich liquid. Reproduced from [234], with the permission of AIP Publishing.

## 7. Exotic gels in real space

Most of what we have discussed pertains to real space analysis of gels formed in colloid–polymer mixtures. While these have received the lion’s share of the attention, gels analysed in real space take many forms. Sometimes the behaviour is similar, sometimes it is profoundly different. Given the nature of spinodal gelation, among the more surprising systems to undergo gelation is polydisperse hard rods (without any appreciable attraction between the particles) [28]. Ferreiro-Córdova and co-workers used real space analysis of a model system of polydisperse hard rods to demonstrate such *non-sticky gelation*. These sepiolite colloidal rods exhibited two important features. Firstly, any attractions were small that they could be accurately modelled as hard rods secondly, the rods are rather polydisperse (with an effective aspect ratio  $\langle L'/D' \rangle = 24.6 \pm 9.5$ ) leading to a large gap in volume fraction between isotropic and nematic phases at phase coexistence. This large gap in volume fraction meant that the relaxation in the nematic phase was around 1000 times slower than that in the isotropic phase (depending on the direction of motion with respect to the director). This leads to viscoelastic phase separation and, for suitable state points, spinodal decomposition. The four characteristics of spinodal gelation noted in the introduction are then met. Such a gel of hard particles is shown in figure 23(a) and computer simulation with similar behaviour revealing local rod orientation in (b).

Bijels are formed for two demixing liquids [237]. However, a novel mechanism is used to prevent full demixing. The bijel is formed by the interface between the two liquids—to which colloids are strongly absorbed, as in a pickering emulsion. Since full phase separation leads to a loss of interfacial area, if one can arrest the decrease in interfacial area between

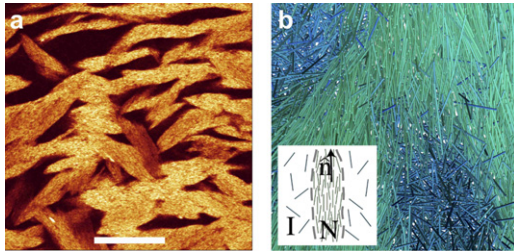


**Figure 23.** Non-sticky spinodal gelation in polydisperse hard rods. Spinodal decomposition leads to a bicontinuous network of isotropic (I) and nematic (N). (a) Confocal image of gel at rod volume fraction  $\phi = 0.043$ , bright regions of nematic phase. Scale bar represents  $4\mu\text{m}$ . (b) Snapshot of a thin slice of a simulation box of rods at  $\phi = 0.140$ . The colours indicate the local order parameter of each rod and range from dark blue for rods in the isotropic phase to bright green for the nematic. Inset shows that rods align parallel to the director, indicated as  $\hat{\mathbf{n}}$ . We expect that the viscosity parallel to the director is low enough to permit flow, while perpendicular flow is strongly suppressed. Reproduced from [28]. CC BY 4.0.

the two phases, a gel-like material can be formed. The interfacial area is then fixed by (2D) close packing of colloids which are strongly absorbed to it. Such a *bijel* is shown schematically in figure 24(a) [235].

Hegelson and co-workers used *polymer bridging* of emulsion droplets as a mechanism to drive colloidal gelation [34]. Here the ‘sticky ends’ of the triblock copolymer tend to be absorbed by two neighbouring emulsion droplets, so that the polymer effectively bridges the droplets. Similar mechanisms had been developed by Porte and co-workers at a much smaller lengthscale [238]. Binary gels between poly(N-isopropylacrylamide) (pNIPAM) microgels and triblock-copolymer surfactant have been investigated by Fussell and co-workers (figure 24(b)), these gels only form at temperatures above the collapse temperature of the microgels. This results in the ability to form gels reversibly with heating. The gelation is caused by the temperature responsive association (i.e. bridging) of the microgel colloids and triblock-copolymer, driven at elevated temperatures by hydrophobic interactions [35, 239].

An exciting development in the context of designing nano-architectures was the work of Varrato and co-workers [236]. Here a binary colloidal system with controllable *specific* interactions (unlike polymer-induced depletion which ‘sticks everything to everything’—see section 6) was designed using DNA-coated colloids. The interactions in the binary system were designed such that each species was attracted to itself, but there was no significant attraction between the two species. Thus, the simultaneous formation of two independent networks in the same suspension was possible, as shown in figure 24(c). Similar behaviour has since been obtained in protein gels [240].

*Protein gels*—we have noted that proteins can form gels. Often the small lengthscales of proteins have led to scattering studies being carried out [12, 151–155]. However, fluorescent proteins are amenable to real space analysis [240]. It is thought that the mechanism of gelation in proteins is often similar to that discussed here [12]. However, the interactions of protein molecules are far more complex, enabling novel

assembly pathways to be designed. In figure 24(d) we show a gel of the fluorescent proteins eGFP and mCherry, whose interactions have been tailored such that the size of domains of each protein can be controlled. Notably, because here the proteins retained their fluorescence, we may infer that they retain their functionality, with potential for the assembly of novel nanomaterials [14]. Very recently, depletion driven gelation in a protein system has been quantitatively mapped to a colloid–polymer model. Given the usually complex nature of protein–protein interactions, mapping of eGFP dimers to hard spherocylinders was thought to be possible due to polymer-induced passivation which led the protein molecules to interact more like hard particles [241].

*Active gels*—active gels of actin tubules form a fascinatingly rich system [41]. Our opinion is that the underlying physics is so different to the systems considered here that we refer the reader to the appropriate literature [242, 243]. However, recently, colloidal gel-like assembly has been achieved with in experiments active colloids with dipolar interactions figure 24(e) [42] and computer simulation of active particles with Lennard-Jones interactions [244]. The former feature a steady-state ‘labyrinthine’ structure which is reminiscent of a transient state of the passive dipolar system [245].

## 8. Outlook

We close with some conclusions about what has been learned and identify some open questions. We begin with what we understand.

- Perhaps surprisingly, given that colloidal systems are prized as simple models, it proved more challenging than expected to realise the simplest colloidal gelformer, sticky spheres in experimental systems suitable for real space analysis with index and in particular density matching (section 4.1). That now seems to be under control, but care should be exercised when preparing experimental systems: it is harder than it seems.
- We understand the mechanisms of how a rigid network emerges from spinodal decomposition, see sections 4.3 and 5.1. Rigidity seems largely geometric and we emphasise the role of hydrodynamics in the early stages of aggregation.
- Beyond these broad statements, a comprehensive analysis of means of identifying rigidity would be highly desirable. In this way, the different characterisation methods might be compared and contrasted in a meaningful manner.

Moving to open questions, loosely speaking it seems that we understand how gels form. Much less clear is what happens next.

- How do gels fail? In the quiescent case (section 5.3), small systems collapse rapidly, but the delayed collapse phenomenon, important though it is in application, continues to elude our understanding. It is perhaps not the ideal task for real space analysis, suited as the technique is to detailed analysis of *local* phenomena, due to the desire to study the whole sample. While excellent work has been carried out with scattering techniques [246] and

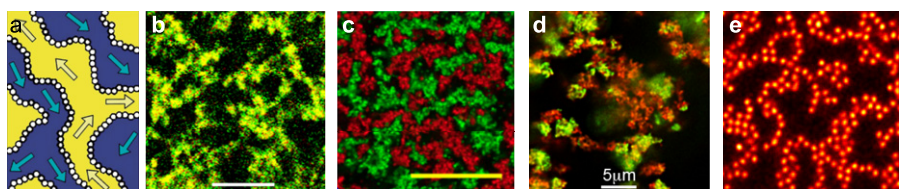


**Figure 24.** Exotic gels and gel-like systems. (a) Schematic geometry of a bijel. The bicontinuous morphology of the bijel allows two immiscible fluids to be passed through the material in opposite directions via a continuous process. Reproduced from [235] with permission of The Royal Society of Chemistry. (b) Confocal images of an example binary gel that forms in mixtures of pNIPAM microgels (3 wt%) and triblock-copolymer (3 wt%) at elevated temperatures, the combined signal from the fluorescein labelled microgels and Nile red labelled triblock-copolymer is shown. Images are taken at 50°C, bar = 10  $\mu\text{m}$ . Reproduced from [35] with permission of The Royal Society of Chemistry. (c) Bigel of binary colloidal system with specific DNA-mediated interactions assembled into two independent networks. Bar = 25  $\mu\text{m}$ . Reproduced from [236]. CC BY 4.0. (d) Binary protein gel with tunable domain sizes [14]. (e) Labyrinth topology in active dipolar gel [42].

computer simulation can yield much insight [55, 56, 247, 248], one cannot help but feel that real space analysis is nevertheless a good way to pinpoint the origins of this phenomenon, perhaps combined with magnetic resonance imaging [221].

- Although investigations have been made (section 5.5), a consensus on how the ‘arms’ of a gel fail seems to be lacking. A detailed, particle-resolved analysis of this process, even in perhaps a somewhat artificial set up, would be most useful.
- The response to shear may provide a good starting point to tackle gel failure. Whether failure mechanisms under shear are the same as those in a gravitational field is unclear, but at least shear provides a means to ‘cause’ failure in such a way that it can be analysed in a reasonably straightforward manner. It may be possible to build on this and use theoretical approaches such as soft glassy rheology [111] or elastoplastic models [113] which may access the relevant timescales (hours to years) and system sizes (at least  $10^{12}$  particles) pertinent to delayed collapse which currently lie outwith the reach of computer simulation of particles.
- The potential of computer simulation of particle-based for improving our understanding of gelation lies, if not in the system sizes and timescales, rather in its precision. This is exemplified in the work of van Doorn *et al* [191] where local mechanisms for failure are investigated in an idealised set-up. Other possibilities include the use of advanced sampling techniques to address the challenges of timescales of up to years important for example in gel failure. However, gels age during this time, rather more obviously than do glasses, for example. One expects that, given a suitable order parameter for ageing techniques like forward flux sampling may be one way to generate gels which have been ‘aged’ in an accelerated manner [249].
- What is the nature of the colloidal glass which leads to the arrest of the phase separation? In recent years, evidence has emerged for a *Gardner transition* in hard sphere glasses between a stable (thermal) glass and a marginal glass or ‘Gardner phase’, depending on the compression rate [76, 250]. The volume fraction of the ‘arms’ of the gel has been determined as  $\phi_c \approx 0.60$  [48, 78], which

may place the system in the Gardner phase, with notable consequences for the mechanical properties [76].

- We may expect to see more exotic systems. It is notable and perhaps remarkable that the vast majority of work reviewed here has concerned the polymethyl methacrylate–polystyrene system (see section 4.2). This is a most amenable system for study, but surely others are suitable, and an obvious candidate would seem to be soft colloids, e.g. microgels [35]. Furthermore, although the colloidal ‘rocks’ (figures 24(d)–(g)) share some characteristics [233], as yet there is no particle-resolved work on ‘empty liquids’ [21], with their intriguing dynamic behaviour [20]. While such systems do not necessarily undergo spinodal gelation and indeed thermodynamically, their behaviour is more akin to that of network glassformers like silica than the systems we have discussed here (see section 4.1 and figure 8), it would certainly be interesting to explore empty liquids in real space used ‘patchy particle’ systems.
- The age of dynamic arrest of active colloids is in its infancy [251], and we expect to see more. Meanwhile the protein gels in figure 24(d) raise the following question: if proteins may be naively thought of as sticky spheres, then why is that protein gels have ‘arms’ on the same lengthscale as colloidal gels when the molecules are a thousand times smaller in diameter. That is to say, a lengthscale of a few microns corresponds to a few ( $< 10$ ) colloid diameters while that same lengthscale corresponds to thousands of protein molecules. How is it that if proteins and colloids somehow obey the same physics (here), then why such a massive difference in lengthscale (in units of the diameter)? It is tempting to speculate that because proteins are so much smaller, and the Brownian time  $\tau_B \sim \sigma^3$ , then in a sense, time runs  $10^9$  times faster in the case of proteins. So we are looking at a gel at a much later stage than is the case with the colloids—for the same laboratory timescale. Such speculations of course warrant careful investigation.

We close by concluding that in the 18 years since the pioneering work of Dinsmore and Weitz [117] a great deal has been done with real space analysis of colloidal gels, and many open questions remain.

## Acknowledgments

In connection with the preparation of this article, and for enlightening discussions pertaining to gelation, the authors would like to thank Dirk Aarts, Ludovic Berthier, Paul Bartlett, Daniel Bonn, Patrick Charbonneau, Rui Cheng, Luca Cipeletti, Marjolein Dijkstra, Roel Dullens, Jeroen van Duijnveldt, Stefan Egelhaaf, Bob Evans, Jens Eggers, Claudia Ferreiro-Córdova, Giuseppe Foffi, Sharon Glotzer, Peter Harrowell, Lilian Hsiao, Rob Jack, Willem Kegel, Christian Klix, Tannie Liverpool, Henk Lekkerkerker, Mattieu Leocmach, Hartmut Löwen, Jennifer Mcmanus, Kuni Miyazaki, Takehiro Ohtsuka, Rattachai Pinchiapat, Wilson Poon, Itamar Procaccia, Azaima Razali, Rebecca Rice, Ioatzin Rios de Anda, David Richard, Roland Roth, John Russo, Nariaki Saka, Peter Schall Francesco Sciortino, Mike Solomon, Ken Schweizer, Thomas Speck, Grzegorz Szamel, Hajime Tanaka, Shelley Taylor, Francesco Turci, Brian Vincent, Eric Weeks, Nigel Wilding, Stephen Williams, Emanuela Zaccarelli, Alessio Zaccone Isla Zhang and Roseanna Zia. CPR gratefully acknowledges the Royal Society and EPSRC Grant EP/T031077/1. CPR and JEH acknowledge European Research Council (ERC Consolidator Grant NANOPRS, Project Number 617266). SLF is supported by a studentship provided by the Bristol Centre for Functional Nanomaterials (EPSRC Grant EP/L016648/1). CPR and MAF gratefully acknowledge support from Bayer AG.

## Data availability statement

No new data were created or analysed in this study.

## ORCID iDs

C Patrick Royall  <https://orcid.org/0000-0001-7247-8685>  
 Sian L Fussell  <https://orcid.org/0000-0002-2462-2440>  
 James E Hallett  <https://orcid.org/0000-0002-9747-9980>

## References

- [1] Tanaka H 2000 Viscoelastic phase separation *J. Phys.: Condens. Matter.* **12** R207–64
- [2] Poon W C K 2002 The physics of a model colloid polymer mixture *J. Phys.: Condens. Matter.* **14** R859
- [3] Cipelletti L and Ramos L 2005 Slow dynamics in glassy soft matter *J. Phys.: Condens. Matter.* **17** R253–85
- [4] Coniglio A, De Arcangelis L, Del Gado E, Fierro A and Sator N 2004 Percolation, gelation and dynamical behaviour in colloids *J. Phys.: Condens. Matter.* **16** S4831–9
- [5] Zaccarelli E 2007 Colloidal gels: equilibrium and non-equilibrium routes *J. Phys.: Condens. Matter.* **19** 323101
- [6] Drury J L and Mooney D J 2003 Hydrogels for tissue engineering: scaffold design variables and applications *Biomaterials* **24** 4337–51
- [7] Rose S, Preveteau A, Elzière P, Hourdet D, Marcellan A and Leibler L 2014 Nanoparticle solutions as adhesives for gels and biological tissues *Nature* **505** 382–5
- [8] Ubbink J 2012 Soft matter approaches to structured foods: from ‘cook-and-look’ to rational food design? *Faraday Discuss.* **158** 9
- [9] Liang J, Ma Y, Zheng Y, Davis H T, Chang H-T, Binder D, Abbas S and Hsu F-L 2001 Solvent-induced crystal morphology transformation in a ternary soap system: sodium stearate crystalline fibers and platelets *Langmuir* **17** 6447–54
- [10] Cardinaux F, Gibaud T, Stradner A and Schurtenberger P 2007 Interplay between spinodal decomposition and glass formation in proteins exhibiting short-range attractions *Phys. Rev. Lett.* **99** 118301
- [11] Leocmach M, Perge C, Divoux T and Manneville S 2014 Creep and fracture of a protein gel under stress *Phys. Rev. Lett.* **113** 038303
- [12] McManus J J, Charbonneau P, Zaccarelli E and Asherie N 2016 The physics of protein self-assembly *Curr. Opin. Colloid Interface Sci.* **22** 73–9
- [13] Fusco D and Charbonneau P 2016 Soft matter perspective on protein crystal assembly *Colloids Surf. B* **137** 22–31
- [14] Rios de Anda I, Coutable-Pennarun A, Brasnett C, Whitelam S, Seddon A, Russo J, Ross Anderson J L and Royall C P 2019 Decorated protein networks: functional nanomaterials with tunable domain size (arXiv:[1911.05857](https://arxiv.org/abs/1911.05857) [Cond-Mat Physicsphysics Q-Bio])
- [15] Ulrich S, Aspelmeier T, Roeller K, Fingerle A, Herminghaus S and Zippelius A 2009 Cooling and aggregation in wet granulates *Phys. Rev. Lett.* **102** 148002
- [16] Li J, Cao Y, Xia C, Kou B, Xiao X, Fezzaa K and Wang Y 2014 Similarity of wet granular packing to gels *Nat. Commun.* **5** 5014
- [17] Bouttes D, Gouillart E, Boller E, Dalmas D and Vandembroucq D 2014 Fragmentation and limits to dynamical scaling in viscous coarsening: an interrupted *in situ* x-ray tomographic study *Phys. Rev. Lett.* **112** 245701
- [18] Baumer R E and Demkowicz M J 2013 Glass transition by gelation in a phase separating binary alloy *Phys. Rev. Lett.* **110** 145502
- [19] Ruzicka B, Zaccarelli E, Julian L, Angelini R, Sztucki M, Moussaïd A, Narayanan T and Sciortino F 2011 Observation of empty liquids and equilibrium gels in a colloidal clay *Nat. Mater.* **10** 56–60
- [20] Saika-Voivod I, King H M, Tartaglia P, Sciortino F and Zaccarelli E 2011 Silica through the eyes of colloidal models—when glass is a gel *J. Phys.: Condens. Matter.* **23** 285101
- [21] Bianchi E, Largo J, Tartaglia P, Zaccarelli E and Sciortino F 2006 Phase diagram of patchy colloids: towards empty liquids *Phys. Rev. Lett.* **97** 168301
- [22] Jabbari-Farouji S, Wegdam G H and Bonn D 2007 Gels and glasses in a single system: evidence for an intricate free-energy landscape of glassy materials *Phys. Rev. Lett.* **99** 065701
- [23] Onuki A 2002 *Phase Transition Dynamics* (Cambridge: Cambridge University Press)
- [24] Lekkerkerker H N W, Poon W C-K, Pusey P N, Stroobants A and Warren P B 1992 Phase behaviour of colloid + polymer mixtures *Europhys. Lett.* **20** 559–64
- [25] Teece L J, Faers M A and Bartlett P 2011 Ageing and collapse in gels with long-range attractions *Soft Matter* **7** 1341–51
- [26] Klotsa D and Jack R L 2011 Predicting the self-assembly of a model colloidal crystal *Soft Matter* **7** 6294
- [27] Whitelam S and Jack R L 2015 The statistical mechanics of dynamic pathways to self-assembly *Annu. Rev. Phys. Chem.* **66** 143–63
- [28] Ferreiro-Córdova C, Royall C P and van Duijneveldt J S 2020 Anisotropic viscoelastic phase separation in polydisperse hard rods leads to nonsticky gelation *Proc. Natl Acad. Sci. USA* **117** 3415–20
- [29] Russel W, Saville D and Schowalter W 1989 *Colloidal Dispersions* (Cambridge: Cambridge University Press)
- [30] Weitz D A and Oliveria M 1984 Fractal structures formed by kinetic aggregation of aqueous gold colloids *Phys. Rev. Lett.* **52** 1433–6

- [31] Asakura S and Oosawa F 1954 On interaction between two bodies immersed in a solution of macromolecules *J. Chem. Phys.* **22** 1433–6
- [32] Long J A, Osmond D W J and Vincent B 1976 The equilibrium aspects of weak flocculation *J. Colloid Interface Sci.* **42** 545
- [33] Appell J, Porte G and Rawiso M 1998 Interactions between nonionic surfactant micelles introduced by a telechelic polymer. A small angle neutron scattering study *Langmuir* **14** 4409–14
- [34] Gao Y 2015 Microdynamics and arrest of coarsening during spinodal decomposition in thermoreversible colloidal gels *Soft Matter* **11** 6360–70
- [35] Fussell S L, Bayliss K, Coops C, Matthews L, Li W, Briscoe W H, Faers M A, Royall C P and van Duijneveldt J S 2019 Reversible temperature-controlled gelation in mixtures of pNIPAM microgels and non-ionic polymer surfactant *Soft Matter* **15** 8578–88
- [36] Veen S J, Antoniuk O, Weber B, Potenza M A C, Mazzoni S, Schall P and Wegdam G H 2012 Colloidal aggregation in microgravity by critical Casimir forces *Phys. Rev. Lett.* **109** 248302
- [37] Hertlein C, Helden L, Gambassi A, Dietrich S and Bechinger C 2008 Direct measurement of critical Casimir forces *Nature* **451** 172–5
- [38] Bonn D, Otwinowski J, Sacanna S, Guo H, Wegdam G and Schall P 2009 Direct observation of colloidal aggregation by critical Casimir forces *Phys. Rev. Lett.* **103** 156101
- [39] Rouwhorst J, Ness C, Stoyanov S, Zaccone A and Schall P 2020 Nonequilibrium continuous phase transition in colloidal gelation with short-range attraction *Nat. Commun.* **11** 3558
- [40] Rouwhorst J, Schall P, Ness C, Blijdenstein T and Zaccone A 2020 Nonequilibrium master kinetic equation modeling of colloidal gelation *Phys. Rev. E* **102** 022602
- [41] DeCamp S J, Redner G S, Baskaran A, Hagan M F and Dogic Z 2015 Orientational order of motile defects in active nematics *Nat. Mater.* **14** 1110–5
- [42] Sakaï N and Royall C P 2020 Active dipolar colloids in three dimensions: strings, sheets, labyrinthine textures and crystals (arXiv:2010.03925 [Cond-Mat Physicsphysics])
- [43] Ivlev A, Lowen H, Morfill G E and Royall C P 2012 *Complex Plasmas and Colloidal Dispersions: Particle-Resolved Studies of Classical Liquids and Solids* (Singapore: World Scientific)
- [44] The perceived wisdom of materials science is that the microscopic structure determines the dynamics and macroscopic behaviour of the material. Attributed to Peter Harrowell
- [45] Baxter R J 1968 Percus–Yevick equation for hard spheres with surface adhesion *J. Chem. Phys.* **49** 2770–4
- [46] Miller M A and Frenkel D 2003 Competition of percolation and phase separation in a fluid of adhesive hard spheres *Phys. Rev. Lett.* **90** 135702
- [47] Pham K N 2002 Multiple glassy states in a simple model system *Science* **296** 104–6
- [48] Royall C P, Williams S R and Tanaka H 2018 Vitrification and gelation in sticky spheres *J. Chem. Phys.* **148** 044501
- [49] Foffi G, Dawson K A, Buldyrev S V, Sciortino F, Zaccarelli E and Tartaglia P 2002 Evidence for an unusual dynamical-arrest scenario in short-ranged colloidal systems *Phys. Rev. E* **65** 050802
- [50] Bergenholz J, Poon W C K and Fuchs M 2003 Gelation in model colloid–polymer mixtures *Langmuir* **19** 4493–503
- [51] Chen Y-L and Schweizer K S 2004 Microscopic theory of gelation and elasticity in polymer-particle suspensions *J. Chem. Phys.* **120** 7212–22
- [52] Shah S A, Chen Y-L, Ramakrishnan S, Schweizer K S and Zukoski C F 2003 Microstructure of dense colloid–polymer suspensions and gels *J. Phys.: Condens. Matter* **15** 4751–78
- [53] Buscall R and White L R 1987 The consolidation of concentrated suspensions. Part 1—the theory of sedimentation *J. Chem. Soc. Faraday Trans. I* **83** 873
- [54] Zaccone A, Wu H and Del Gado E 2009 Elasticity of arrested short-ranged attractive colloids: homogeneous and heterogeneous glasses *Phys. Rev. Lett.* **103** 208301
- [55] Puertas A M, Fuchs M and Cates M E 2004 Dynamical heterogeneities close to a colloidal gel *J. Chem. Phys.* **121** 2813
- [56] Padmanabhan P and Zia R 2018 Gravitational collapse of colloidal gels: non-equilibrium phase separation driven by osmotic pressure *Soft Matter* **14** 3265–87
- [57] Del Gado E, Fierro A, de Arcangelis L and Coniglio A 2003 A unifying model for chemical and colloidal gels *Europhys. Lett.* **63** 1–7
- [58] Berthier L and Biroli G 2011 Theoretical perspective on the glass transition and amorphous materials *Rev. Mod. Phys.* **83** 587–645
- [59] Manley S *et al* 2005 Time-dependent strength of colloidal gels *Phys. Rev. Lett.* **95** 048302
- [60] Krishna Reddy N, Zhang Z, Paul Lettinga M, Dhont J K G and Vermant J 2012 Probing structure in colloidal gels of thermoreversible rodlike virus particles: rheology and scattering *J. Rheol.* **56** 1153–74
- [61] Faers M A, Choudhury T H, Lau B, McAllister K and Luckham P F 2006 Syneresis and rheology of weak colloidal particle gels *Colloids Surf. A* **288** 170–9
- [62] Starrs L, Poon W C K, Hibberd D J and Robins M M 2002 Collapse of transient gels in colloid–polymer mixtures *J. Phys.: Condens. Matter* **14** 2485–505
- [63] Bartlett P, Teece L J and Faers M A 2012 Sudden collapse of a colloidal gel *Phys. Rev. E* **85** 021404
- [64] Carpineti M and Giglio M 1992 Spinodal-type dynamics in fractal aggregation of colloidal clusters *Phys. Rev. Lett.* **68** 3327–30
- [65] Cipelletti L, Manley S, Ball R C and Weitz D A 2000 Universal aging features in the restructuring of fractal colloidal gels *Phys. Rev. Lett.* **84** 2275–8
- [66] Verhaegh N A M, Asnagh D and Lekkerkerker H N W 1999 Transient gels in colloid–polymer mixtures studied with fluorescence confocal scanning laser microscopy *Physica A* **264** 64–74
- [67] Chaikin P M and Lubeneksy T C 1995 *Principles of Condensed Matter Physics* (Cambridge: Cambridge University Press)
- [68] Cahn J W and Hilliard J E 1959 Free energy of a nonuniform system. III. Nucleation in a two-component incompressible fluid *J. Chem. Phys.* **31** 688–99
- [69] Cavagna A 2009 Supercooled liquids for pedestrians *Phys. Rep.* **476** 51–124
- [70] Royall C P and Williams S R 2015 The role of local structure in dynamical arrest *Phys. Rep.* **560** 1–75
- [71] Royall C P, Turci F, Tatsumi S, Russo J and Robinson J 2018 The race to the bottom: approaching the ideal glass? *J. Phys.: Condens. Matter* **30** 363001
- [72] Berthier L and Ediger M D 2016 Facets of glass physics *Phys. Today* **69** 40–6
- [73] Biroli G and Garrahan J P 2013 Perspective: the glass transition *J. Chem. Phys.* **138** 12A301
- [74] Debenedetti P G and Stillinger F H 2001 Supercooled liquids and the glass transition *Nature* **410** 259–67
- [75] Royall C P, Turci F and Speck T 2020 Dynamical phase transitions and their relation to structural and thermodynamic aspects of glass physics *J. Chem. Phys.* **153** 090901
- [76] Charbonneau P, Kurchan J, Parisi G, Urbani P and Zamponi F 2017 Glass and jamming transitions: from exact results to finite-dimensional descriptions *Annu. Rev. Condens. Matter Phys.* **8** 265–88
- [77] Manley S, Wyss H M, Miyazaki K, Conrad J C, Trappe V, Kaufman L J, Reichman D R and Weitz D A 2005 Glasslike

- arrest in spinodal decomposition as a route to colloidal gelation *Phys. Rev. Lett.* **95** 238302
- [78] Lu P J, Zaccarelli E, Ciulla F, Schofield A B, Sciortino F and Weitz D A 2008 Gelation of particles with short-range attraction *Nature* **453** 499–503
- [79] Zaccarelli E, Lu P J, Ciulla F, Weitz D A and Sciortino F 2008 Gelation as arrested phase separation in short-ranged attractive colloid–polymer mixtures *J. Phys.: Condens. Matter* **20** 494242
- [80] Griffiths S, Turci F and Royall C P 2017 Local structure of percolating gels at very low volume fractions *J. Chem. Phys.* **146** 014905
- [81] Jamie E A G, Dullens R P A and Aarts D G A L 2012 Spinodal decomposition of a confined colloid–polymer system *J. Chem. Phys.* **137** 204902
- [82] Fullerton C J and Berthier L 2020 Glassy behaviour of sticky spheres: what lies beyond experimental timescales? (arXiv:2007.14165 [Cond-Mat])
- [83] Gao Y and Kilfoil M L 2007 Direct imaging of dynamical heterogeneities near the colloid-gel transition *Phys. Rev. Lett.* **99** 078301
- [84] Dibble C J, Kogan M and Solomon M J 2008 Structural origins of dynamical heterogeneity in colloidal gels *Phys. Rev. E* **77** 050401R
- [85] Royall C P, Williams S R, Ohtsuka T and Tanaka H 2008 Direct observation of a local structural mechanism for dynamic arrest *Nat. Mater.* **7** 556–61
- [86] Zhang I, Royall C P, Faers M A and Bartlett P 2013 Phase separation dynamics in colloid–polymer mixtures: the effect of interaction range *Soft Matter* **9** 2076
- [87] van Blaaderen A and Wiltzius P 1995 Real-space structure of colloidal hard-sphere glasses *Science* **270** 1177–9
- [88] Weeks E R, Crocker J C, Levitt A C, Schofield A and Weitz D A 2000 Three-dimensional direct imaging of structural relaxation near the colloidal glass transition *Science* **287** 627
- [89] Hallett J E, Turci F and Royall C P 2020 The devil is in the details: pentagonal bipyramids and dynamic arrest *J. Stat. Mech.* **014001**
- [90] Kuhn T S 1962 *The Structure of Scientific Revolutions* (Chicago: University of Chicago Press)
- [91] Goetze W 2009 *Complex Dynamics of Glass-Forming Liquids: A Mode-Coupling Theory* (Oxford: Oxford University Press)
- [92] Reichman D R and Charbonneau P 2005 Mode-coupling theory *J. Stat. Mech.* **P05013**
- [93] Brambilla G, El Masri D, Pierro M, Berthier L, Cipelletti L, Petekidis G and Schofield A B 2009 Probing the equilibrium dynamics of colloidal hard spheres above the mode-coupling glass transition *Phys. Rev. Lett.* **102** 085703
- [94] Hallett J E, Turci F and Royall C P 2018 Local structure in deeply supercooled liquids exhibits growing lengthscales and dynamical correlations *Nat. Commun.* **9** 3272
- [95] Janssen L M C and Reichman D R 2015 Microscopic dynamics of supercooled liquids from first principles *Phys. Rev. Lett.* **115** 205701
- [96] Adam G and Gibbs J H 1965 On the temperature dependence of relaxation phenomena in glass-forming liquids *J. Chem. Phys.* **43** 139–46
- [97] Lubchenko V and Wolynes P G 2007 Theory of structural glasses and supercooled liquids *Annu. Rev. Phys. Chem.* **58** 235–66
- [98] Parisi G and Zamponi F 2010 Mean-field theory of hard sphere glasses and jamming *Rev. Mod. Phys.* **82** 57
- [99] Tarjus G, Kivelson S A, Nussinov Z and Viot P 2005 The frustration-based approach of supercooled liquids and the glass transition: a review and critical assessment *J. Phys.: Condens. Matter* **17** R1143–82
- [100] Chandler D and Garrahan J P 2010 Dynamics on the way to forming glass: bubbles in space-time *Annu. Rev. Phys. Chem.* **61** 191–217
- [101] Turci F, Royall C P and Speck T 2017 Nonequilibrium phase transition in an atomistic glassformer: the connection to thermodynamics *Phys. Rev. X* **7** 031028
- [102] Hecksher T, Nielsen A I, Olsen N B and Dyre J C 2008 Little evidence for dynamic divergences in ultraviscous molecular liquids *Nat. Phys.* **4** 737–41
- [103] Ozawa M, Scalliet C, Ninarello A and Berthier L 2019 Does the Adam-Gibbs relation hold in simulated supercooled liquids? *J. Chem. Phys.* **151** 084504
- [104] Cates M E, Fuchs M, Kroy K, Poon W C K and Puertas A M 2004 Theory and simulation of gelation, arrest and yielding in attracting colloids *J. Phys.: Condens. Matter* **16** S4861–75
- [105] Ball R C, Weitz D A, Witten T A and Leyvraz F 1987 Universal kinetics in reaction-limited aggregation *Phys. Rev. Lett.* **58** 274–7
- [106] Kroy K, Cates M E and Poon W C K 2004 Cluster mode-coupling approach to weak gelation in attractive colloids *Phys. Rev. Lett.* **92** 148302
- [107] Eberle A P R, Wagner N J and Castañeda-Priego R 2011 Dynamical arrest transition in nanoparticle dispersions with short-range interactions *Phys. Rev. Lett.* **106** 105704
- [108] Laurati M, Petekidis G, Koumakis N, Cardinaux F, Schofield A B, Brader J M, Fuchs M and Egelhaaf S U 2009 Structure, dynamics, and rheology of colloid–polymer mixtures: from liquids to gels *J. Chem. Phys.* **130** 134907
- [109] Gopalakrishnan V, Schweizer K S and Zukoski C F 2006 Linking single particle rearrangements to delayed collapse times in transient depletion gels *J. Phys.: Condens. Matter* **18** 11531–50
- [110] Mewis J and Wagner N J 2009 Thixotropy *Adv. Colloid Interface Sci.* **147–148** 214–27
- [111] Fielding S M 2014 Shear banding in soft glassy materials *Rep. Prog. Phys.* **77** 102601
- [112] Bonn D, Denn M M, Berthier L, Divoux T and Manneville S 2017 Yield stress materials in soft condensed matter *Rev. Mod. Phys.* **89** 035005
- [113] Nicolas A, Ferrero E E, Martens K and Barrat J-L 2018 Deformation and flow of amorphous solids: insights from elastoplastic models *Rev. Mod. Phys.* **90** 045006
- [114] Dijkstra M, Brader J M and Evans R 1999 Phase behaviour and structure of model colloid–polymer mixtures *J. Phys.: Condens. Matter* **11** 10079–106
- [115] Dijkstra M, van Roij R and Evans R 2000 Effective interactions, structure, and isothermal compressibility of colloidal suspensions *J. Chem. Phys.* **113** 9
- [116] Taffs J, Malins A, Williams S R and Royall C P 2010 A structural comparison of models of colloid–polymer mixtures *J. Phys.: Condens. Matter* **22** 104119
- [117] Dinsmore A D and Weitz D A 2002 Direct imaging of three-dimensional structure and topology of colloidal gels *J. Phys.: Condens. Matter* **14** 7581–97
- [118] Hunter G L and Weeks E R 2012 The physics of the colloidal glass transition *Rep. Prog. Phys.* **75** 066501
- [119] Lu P J and Weitz D A 2013 Colloidal particles: crystals, glasses, and gels *Annu. Rev. Condens. Matter Phys.* **4** 217–33
- [120] Yunker P J, Chen K, Gratale M D, Lohr M A, Still T and Yodh A G 2014 Physics in ordered and disordered colloidal matter composed of poly(N-isopropylacrylamide) microgel particles *Rep. Prog. Phys.* **77** 056601
- [121] van Blaaderen A, Imhof A, Hage W and Vrij A 1992 Three-dimensional imaging of submicrometer colloidal particles in concentrated suspensions using confocal scanning laser microscopy *Langmuir* **8** 1514–7

- [122] Gasser U 2001 Real-space imaging of nucleation and growth in colloidal crystallization *Science* **292** 258–62
- [123] Taffs J, Williams S R, Tanaka H and Royall C P 2013 Structure and kinetics in the freezing of nearly hard spheres *Soft Matter* **9** 297–305
- [124] Crocker J C and Grier D G 1996 Methods of digital video microscopy for colloidal studies *J. Colloid Interface Sci.* **179** 298–310
- [125] Leocmach M and Tanaka H 2013 A novel particle tracking method with individual particle size measurement and its application to ordering in glassy hard sphere colloids *Soft Matter* **9** 1447–57
- [126] Gao Y and Kilfoil M L 2009 Accurate detection and complete tracking of large populations of features in three dimensions *Opt. Express* **17** 4685
- [127] Bierbaum M, Leahy B D, Alemi A A, Cohen I and Sethna J P 2017 Light microscopy at maximal precision *Phys. Rev. X* **7** 041007
- [128] Kurita R, Ruffner D B and Weeks E R 2012 Measuring the size of individual particles from three-dimensional imaging experiments *Nat. Commun.* **3** 1127
- [129] Koenderink G H, Vliegenthart G A, Kluijtmans S G J M, van Blaaderen A, Philipse A P and Lekkerkerker H N W 1999 Depletion-induced crystallization in colloidal rod–sphere mixtures *Langmuir* **15** 4693–6
- [130] Tolpekin V A, Duits M H G, van den Ende D and Mellema J 2004 Aggregation and breakup of colloidal particle aggregates in shear flow, studied with video microscopy *Langmuir* **20** 2614–27
- [131] de Hoog E H A, Kegel W K, van Blaaderen A and Lekkerkerker H N W 2001 Direct observation of crystallization and aggregation in a phase-separating colloid–polymer suspension *Phys. Rev. E* **64** 021407
- [132] Pusey P N and van Megen W 1986 Phase behaviour of concentrated suspensions of nearly hard colloidal spheres *Nature* **320** 340–2
- [133] Poon W C K, Weeks E R and Royall C P 2012 On measuring colloidal volume fractions *Soft Matter* **8** 21–30
- [134] Royall C P, Poon W C K and Weeks E R 2013 In search of colloidal hard spheres *Soft Matter* **9** 17–27
- [135] Royall C P, van Roij R and van Blaaderen A 2005 Extended sedimentation profiles in charged colloids: the gravitational length, entropy, and electrostatics *J. Phys.: Condens. Matter* **17** 2315–26
- [136] Royall C P, Leunissen M E and van Blaaderen A 2003 A new colloidal model system to study long-range interactions quantitatively in real space *J. Phys.: Condens. Matter* **15** S3581–96
- [137] Klix C L, Royall C P and Tanaka H 2010 Structural and dynamical features of multiple metastable glassy states in a colloidal system with competing interactions *Phys. Rev. Lett.* **104** 165702
- [138] Royall C P 2018 Hunting mermaids in real space: known knowns, known unknowns and unknown unknowns *Soft Matter* **14** 4020–8
- [139] El Masri D *et al* 2012 A qualitative confocal microscopy study on a range of colloidal processes by simulating microgravity conditions through slow rotations *Soft Matter* **8** 6979
- [140] Sedgwick H, Egelhaaf S U and Poon W C K 2004 Clusters and gels in systems of sticky particles *J. Phys.: Condens. Matter* **16** S4913–22
- [141] Campbell A I, Anderson V J, van Duijneveldt J S and Bartlett P 2005 Dynamical arrest in attractive colloids: the effect of long-range repulsion *Phys. Rev. Lett.* **94** 208301
- [142] Yethiraj A and van Blaaderen A 2003 A colloidal model system with an interaction tunable from hard sphere to soft and dipolar *Nature* **421** 513–7
- [143] Rios de Anda I, Statt A, Turci F and Royall C P 2015 Low-density crystals in charged colloids: comparison with Yukawa theory: low-density crystals in charged colloids: comparison with Yukawa theory *Contrib. Plasma Phys.* **55** 172–9
- [144] Leunissen M E, van Blaaderen A, Hollingsworth A D, Sullivan M T and Chaikin P M 2007 Electrostatics at the oil–water interface, stability, and order in emulsions and colloids *Proc. Natl Acad. Sci.* **104** 2585–90
- [145] Dinsmore A D, Prasad V, Wong I Y and Weitz D A 2006 Microscopic structure and elasticity of weakly aggregated colloidal gels *Phys. Rev. Lett.* **96** 185502
- [146] Zhao K and Mason T G 2007 Directing colloidal self-assembly through roughness-controlled depletion attractions *Phys. Rev. Lett.* **99** 268301
- [147] Lu P J, Conrad J C, Wyss H M, Schofield A B and Weitz D A 2006 Fluids of clusters in attractive colloids *Phys. Rev. Lett.* **96** 028306
- [148] Leunissen M E 2006 Manipulating colloids with charge and electric fields *PhD Thesis* Utrecht University, Utrecht
- [149] Royall C P, Aarts D G A L and Tanaka H 2005 Fluid structure in colloid–polymer mixtures: the competition between electrostatics and depletion *J. Phys.: Condens. Matter* **17** S3401–8
- [150] Groenewold J and Kegel W K 2001 Anomalously large equilibrium clusters of colloids *J. Phys. Chem. B* **105** 11702–9
- [151] Stradner A, Sedgwick H, Cardinaux F, Poon W C K, Egelhaaf S U and Schurtenberger P 2004 Equilibrium cluster formation in concentrated protein solutions and colloids *Nature* **432** 492–5
- [152] Stradner A 2020 Potential and limits of a colloid approach to protein solutions *Soft Matter* **16** 307–23
- [153] Bucciarelli S, Casal-Dujat L, De Michele C, Sciortino F, Dhont J, Bergenholz J, Farago B, Schurtenberger P and Stradner A 2015 Unusual dynamics of concentration fluctuations in solutions of weakly attractive globular proteins *J. Phys. Chem. Lett.* **6** 4470–4
- [154] Bucciarelli S *et al* 2016 Dramatic influence of patchy attractions on short-time protein diffusion under crowded conditions *Sci. Adv.* **2** e1601432
- [155] Myung J S, Roosen-Runge F, Winkler R G, Gompper G, Schurtenberger P and Stradner A 2018 Weak shape anisotropy leads to a nonmonotonic contribution to crowding, impacting protein dynamics under physiologically relevant conditions *J. Phys. Chem. B* **122** 12396–402
- [156] Shukla A, Mylonas E, Di Cola E, Finet S, Timmins P, Narayanan T and Svergun D I 2008 Absence of equilibrium cluster phase in concentrated lysozyme solutions *Proc. Natl Acad. Sci.* **105** 5075–80
- [157] Zhang F *et al* 2008 Reentrant condensation of proteins in solution induced by multivalent counterions *Phys. Rev. Lett.* **101** 148101
- [158] van Schooneveld M M, de Villeneuve V W A, Dullens R P A, Aarts D G A L, Leunissen M E and Kegel W K 2009 Structure, stability, and formation pathways of colloidal gels in systems with short-range attraction and long-range repulsion *J. Phys. Chem. B* **113** 4560–4
- [159] Klix C L, Murata K-i, Tanaka H, Williams S R, Malins A and Royall C P 2013 Novel kinetic trapping in charged colloidal clusters due to self-induced surface charge organization *Sci. Rep.* **3** 2072
- [160] Capellmann R F, Valadez-Pérez N E, Simon B, Egelhaaf S U, Laurati M and Castañeda-Priego R 2016 Structure of colloidal gels at intermediate concentrations: the role of competing interactions *Soft Matter* **12** 9303–13
- [161] Ohtsuka T, Royall C P and Tanaka H 2008 Local structure and dynamics in colloidal fluids and gels *Europhys. Lett.* **84** 46002
- [162] Sciortino F, Tartaglia P and Zaccarelli E 2005 One-dimensional cluster growth and branching gels in colloidal

- systems with short-range depletion attraction and screened electrostatic repulsion *J. Phys. Chem. B* **109** 21942–53
- [163] Kohl M, Capellmann R F, Laurati M, Egelhaaf S U and Schmiedeberg M 2016 Directed percolation identified as equilibrium pre-transition towards non-equilibrium arrested gel states *Nat. Commun.* **7** 11817
- [164] Kim J M, Fang J, Eberle A P R, Castañeda-Priego R and Wagner N J 2013 Gel transition in adhesive hard-sphere colloidal dispersions: the role of gravitational effects *Phys. Rev. Lett.* **110** 208302
- [165] Richard D, Royall C P and Speck T 2018 Communication: is directed percolation in colloid–polymer mixtures linked to dynamic arrest? *J. Chem. Phys.* **148** 241101
- [166] Noro M G and Frenkel D 2000 Extended corresponding-states behavior for particles with variable range attractions *J. Chem. Phys.* **113** 2941–4
- [167] van Megen W, Mortensen T C, Williams S R and Müller J 1998 Measurement of the self-intermediate scattering function of suspensions of hard spherical particles near the glass transition *Phys. Rev. E* **58** 6073–85
- [168] Charles Frank F 1952 Supercooling of liquids *Proc. R. Soc. A* **215** 43–6
- [169] Steinhardt P J, Nelson D R and Ronchetti M 1983 Bond-orientational order in liquids and glasses *Phys. Rev. B* **28** 784–805
- [170] Robinson J F, Turci F, Roth R and Royall C P 2019 Morphometric approach to many-body correlations in hard spheres *Phys. Rev. Lett.* **122** 068004
- [171] Meng G, Arkus N, Brenner M P and Manoharan V N 2010 The free-energy landscape of clusters of attractive hard spheres *Science* **327** 560–3
- [172] Malins A, Williams S R, Eggers J, Tanaka H and Royall C P 2009 Geometric frustration in small colloidal clusters *J. Phys.: Condens. Matter.* **21** 425103
- [173] Miller M A, Doye J P K and Wales D J 1999 Structural relaxation in Morse clusters: energy landscapes *J. Chem. Phys.* **110** 328–34
- [174] Doye J P K, Wales D J and Berry R S 1995 The effect of the range of the potential on the structures of clusters *J. Chem. Phys.* **103** 4234–49
- [175] Mossa S and Tarjus G 2003 Locally preferred structure in simple atomic liquids *J. Chem. Phys.* **119** 8069–74
- [176] Taffs J, Malins A, Williams S R and Royall C P 2010 The effect of attractions on the local structure of liquids and colloidal fluids *J. Chem. Phys.* **133** 244901
- [177] Royall C P, Malins A, Dunleavy A J and Pinney R 2015 Strong geometric frustration in model glassformers *J. Non-Cryst. Solids* **407** 34–43
- [178] Malins A, Eggers J, Royall C P, Williams S R and Tanaka H 2013 Identification of long-lived clusters and their link to slow dynamics in a model glass former *J. Chem. Phys.* **138** 12A535
- [179] Malins A, Eggers J, Tanaka H and Royall C P 2013 Lifetimes and lengthscales of structural motifs in a model glassformer *Faraday Discuss.* **167** 405
- [180] Malins A, Williams S R, Eggers J and Royall C P 2013 Identification of structure in condensed matter with the topological cluster classification *J. Chem. Phys.* **139** 234506
- [181] Royall C P, Williams S R, Ohtsuka T, Tanaka H, Tokuyama M, Oppenheim I and Nishiyama H 2008 Direct observation of low-energy clusters in a colloidal gel *AIP Conf. Proc.* vol 982 (AIP) pp 97–101
- [182] Hsiao L C, Newman R S, Glotzer S C and Solomon M J 2012 Role of isostaticity and load-bearing microstructure in the elasticity of yielded colloidal gels *Proc. Natl Acad. Sci.* **109** 16029–34
- [183] Tsurusawa H, Leocmach M, Russo J and Tanaka H 2018 Gelation as condensation frustrated by hydrodynamics and mechanical isostaticity (arXiv:1804.04370 [Cond-Mat])
- [184] Whitaker K A, Varga Z, Hsiao L C, Solomon M J, Swan J W and Furst E M 2019 Colloidal gel elasticity arises from the packing of locally glassy clusters *Nat. Commun.* **10** 2237
- [185] Richard D, Hallett J, Speck T and Royall C P 2018 Coupling between criticality and gelation in ‘sticky’ spheres: a structural analysis *Soft Matter* **14** 5554–64
- [186] Royall C P, Aarts D G A L and Tanaka H 2007 Bridging length scales in colloidal liquids and interfaces from near-critical divergence to single particles *Nat. Phys.* **3** 636–40
- [187] Royall C P, Louis A A and Tanaka H 2007 Measuring colloidal interactions with confocal microscopy *J. Chem. Phys.* **127** 044507
- [188] Hurley M M and Harrowell P 1995 Kinetic structure of a two-dimensional liquid *Phys. Rev. E* **52** 1694–8
- [189] Royall C P, Eggers J, Furukawa A and Tanaka H 2015 Probing colloidal gels at multiple length scales: the role of hydrodynamics *Phys. Rev. Lett.* **114** 258302
- [190] Prasad V, Trappe V, Dinsmore A D, Segre P N, Cipelletti L and Weitz D A 2003 Universal features of the fluid to solid transition for attractive colloidal particles *Faraday Discuss.* **123** 1–12
- [191] van Doorn J M, Verweij J E, Sprakel J and van der Gucht J 2018 Strand plasticity governs fatigue in colloidal gels *Phys. Rev. Lett.* **120** 208005
- [192] Verweij J E, Leermakers F A M, Sprakel J and van der Gucht J 2019 Plasticity in colloidal gel strands *Soft Matter* **15** 6447–54
- [193] Furukawa A and Tanaka H 2010 Key role of hydrodynamic interactions in colloidal gelation *Phys. Rev. Lett.* **104** 245702
- [194] Tsurusawa H, Leocmach M, Russo J and Tanaka H 2019 Direct link between mechanical stability in gels and percolation of isostatic particles *Sci. Adv.* **5** eaav6090
- [195] Manley S *et al* 2004 Limits to gelation in colloidal aggregation *Phys. Rev. Lett.* **93** 108302
- [196] Tsurusawa H, Russo J, Leocmach M and Tanaka H 2017 Formation of porous crystals via viscoelastic phase separation *Nat. Mater.* **16** 1022–8
- [197] Tanaka H, Nishikawa Y and Koyama T 2005 Network-forming phase separation of colloidal suspensions *J. Phys.: Condens. Matter.* **17** L143–53
- [198] Zhang T H, Klok J, Hans Tromp R, Groenewold J and Kegel W K 2012 Non-equilibrium cluster states in colloids with competing interactions *Soft Matter* **8** 667–72
- [199] Royall C P 2018 Kinetic crystallisation instability in liquids with short-ranged attractions *Mol. Phys.* **116** 3076–84
- [200] Royall C P and Malins A 2012 The role of quench rate in colloidal gels *Faraday Discuss.* **158** 301–11
- [201] Sollich P and Wilding N B 2010 Crystalline phases of polydisperse spheres *Phys. Rev. Lett.* **104** 118302
- [202] ten Wolde P R and Frenkel D 1997 Enhancement of protein crystal nucleation by critical density fluctuations *Science* **277** 1975–8
- [203] Savage J R and Dinsmore A D 2009 Experimental evidence for two-step nucleation in colloidal crystallization *Phys. Rev. Lett.* **102** 198302
- [204] Taylor S L, Evans R and Royall C P 2012 Temperature as an external field for colloid–polymer mixtures: ‘quenching’ by heating and ‘melting’ by cooling *J. Phys.: Condens. Matter.* **24** 464128
- [205] Poon W C K and Robins M M 1999 Delayed sedimentation of transient gels in colloid–polymer mixtures : dark-field observation, rheology and dynamic light scattering studies *Faraday Discuss.* **112** 143–54
- [206] Buscall R, Choudhury T H, Faers M A, Goodwin J W, Luckham P A and Partridge S J 2009 Towards rationalising collapse times for the delayed sedimentation of weakly aggregated colloidal gels *Soft Matter* **5** 1345

- [207] Teece L J, Hart J M, Hsu K Y N, Gilligan S, Faers M A and Bartlett P 2014 Gels under stress: the origins of delayed collapse *Colloids Surf. A* **458** 126–33
- [208] Piazza R, Buzzaccaro S and Secchi E 2012 The unbearable heaviness of colloids: facts, surprises, and puzzles in sedimentation *J. Phys.: Condens. Matter* **24** 284109
- [209] Piazza R 2014 Settled and unsettled issues in particle settling *Rep. Prog. Phys.* **77** 056602
- [210] Razali A, Fullerton C J, Turci F, Hallett J E, Jack R L and Royall C P 2017 Effects of vertical confinement on gelation and sedimentation of colloids *Soft Matter* **13** 3230–9
- [211] Kamp S W and Kilfoil M L 2009 Universal behaviour in the mechanical properties of weakly aggregated colloidal particles *Soft Matter* **5** 2438
- [212] Faers M A 2003 The importance of the interfacial stabilising layer on the macroscopic flow properties of suspensions dispersed in non-adsorbing polymer solution *Adv. Colloid Interface Sci.* **106** 23–54
- [213] Laurati M, Egelhaaf S U and Petekidis G 2011 Nonlinear rheology of colloidal gels with intermediate volume fraction *J. Rheol.* **55** 673–706
- [214] Koumakis N, Moghimi E, Besseling R, Poon W C K, Brady J F and Petekidis G 2015 Tuning colloidal gels by shear *Soft Matter* **11** 4640–8
- [215] Smith P A, Petekidis G, Egelhaaf S U and Poon W C K 2007 Yielding and crystallization of colloidal gels under oscillatory shear *Phys. Rev. E* **76** 041402
- [216] Lin N Y C, McCoy J H, Cheng X, Leahy B, Israelachvili J N and Cohen I 2014 A multi-axis confocal rheoscope for studying shear flow of structured fluids *Rev. Sci. Instrum.* **85** 033905
- [217] Isa L, Besseling R and Poon W C K 2007 Shear zones and wall slip in the capillary flow of concentrated colloidal suspensions *Phys. Rev. Lett.* **98** 198305
- [218] Pandey R, Spannuth M and Conrad J C 2014 Confocal imaging of confined quiescent and flowing colloid–polymer mixtures *J. Vis. Exp.* **87** 51461
- [219] Kohl M and Schmiedeberg M 2017 Shear-induced slab-like domains in a directed percolated colloidal gel *Eur. Phys. J. E* **40** 71
- [220] Schwen E M, Ramaswamy M, Cheng C-M, Jan L and Cohen I 2020 Embedding orthogonal memories in a colloidal gel through oscillatory shear *Soft Matter* **16** 3746–52
- [221] Møller P C F, Rodts S, Michels M A J and Bonn D 2008 Shear banding and yield stress in soft glassy materials *Phys. Rev. E* **77** 041507
- [222] Fall A, Paredes J and Bonn D 2010 Yielding and shear banding in soft glassy materials *Phys. Rev. Lett.* **105** 225502
- [223] Sprakler J, Lindström S B, Kodger T E and Weitz D A 2011 Stress enhancement in the delayed yielding of colloidal gels *Phys. Rev. Lett.* **106** 248303
- [224] Han M, Whitmer J K and Luijten E 2019 Dynamics and structure of colloidal aggregates under microchannel flow *Soft Matter* **15** 744–51
- [225] Conrad J C and Lewis J A 2008 Structure of colloidal gels during microchannel flow *Langmuir* **24** 7628–34
- [226] Conrad J C and Lewis J A 2010 Structural evolution of colloidal gels during constricted microchannel flow *Langmuir* **26** 6102–7
- [227] Solomon M J and Spicer P T 2010 Microstructural regimes of colloidal rod suspensions, gels, and glasses *Soft Matter* **6** 1391
- [228] Schilling T, Jungblut S and Miller M A 2007 Depletion-induced percolation in networks of nanorods *Phys. Rev. Lett.* **98** 108303
- [229] Kyrylyuk A V, Hermant M C, Schilling T, Klumperman B, Koning C E and van der Schoot P 2011 Controlling electrical percolation in multicomponent carbon nanotube dispersions *Nat. Nanotechnol.* **6** 364–9
- [230] Lekkerkerker H N W and Tuinier R 2011 *Colloids and the Depletion Interaction (Lecture Notes in Physics vol 833)* (London: Springer)
- [231] Hsiao L C, Schultz B A, Glaser J, Engel M, Szakasits M E, Glotzer S C and Solomon M J 2015 Metastable orientational order of colloidal discoids *Nat. Commun.* **6** 8507
- [232] Wilkins G M H, Spicer P T and Solomon M J 2009 Colloidal system to explore structural and dynamical transitions in rod networks, gels, and glasses *Langmuir* **25** 8951–9
- [233] Rice R, Roth R and Royall C P 2012 Polyhedral colloidal ‘rocks’: low-dimensional networks *Soft Matter* **8** 1163–7
- [234] Zhang I, Pinchaipat R, Wilding N B, Faers M A, Bartlett P, Evans R and Royall C P 2018 Composition inversion in mixtures of binary colloids and polymer *J. Chem. Phys.* **148** 184902
- [235] Cates M E and Clegg P S 2008 Bijels: a new class of soft materials *Soft Matter* **4** 2132
- [236] Varrato F, Di Michele L, Belushkin M, Dorsaz N, Nathan S H, Eiser E and Foffi G 2012 Arrested demixing opens route to bigels *Proc. Natl Acad. Sci.* **109** 19155–60
- [237] Herzig E M, White K A, Schofield A B, Poon W C K and Clegg P S 2007 Bicontinuous emulsions stabilized solely by colloidal particles *Nat. Mater.* **6** 966–71
- [238] Filali M, Ouazzani M J, Michel E, Aznar R, Porte G and Appell J 2001 Robust phase behavior of model transient networks *J. Phys. Chem. B* **105** 10528–35
- [239] Fussell S L, Royall C P and van Duijneveldt J S 2021 Controlling phase separation in microgel-polymeric micelle mixtures using variable quench rates (arXiv:2104.04022 [Cond-Mat])
- [240] Blumlein A and McManus J J 2015 Bigels formed via spinodal decomposition of unfolded protein *J. Mater. Chem. B* **3** 3429–35
- [241] Cheng R, Rios de Anda I, Taylor T W C, Faers M A, Anderson J L R, Seddon A M and Royall C P 2021 Protein–polymer mixtures in the colloid limit: aggregation, sedimentation *J. Chem. Phys.* (arXiv:2106.08974)
- [242] Bechinger C, Di Leonardo R, Löwen H, Reichhardt C, Volpe G and Volpe G 2016 Active particles in complex and crowded environments *Rev. Mod. Phys.* **88** 045006
- [243] Marchetti M C, Joanny J F, Ramaswamy S, Liverpool T B, Prost J, Rao M and Simha R A 2013 Hydrodynamics of soft active matter *Rev. Mod. Phys.* **85** 1143–89
- [244] Prymidis V, Sielcken H and Filion L 2015 Self-assembly of active attractive spheres *Soft Matter* **11** 4158–66
- [245] Dassanayake U, Fraden S and van Blaaderen A 2000 Structure of electrorheological fluids *J. Chem. Phys.* **112** 3851–8
- [246] Aime S, Ramos L and Cipelletti L 2018 Microscopic dynamics and failure precursors of a gel under mechanical load *Proc. Natl Acad. Sci. USA* **115** 3587–92
- [247] Harich R, Blythe T W, Hermes M, Zaccarelli E, Sederman A J, Gladden L F and Poon W C K 2016 Gravitational collapse of depletion-induced colloidal gels *Soft Matter* **12** 4300–8
- [248] Varga Z and Swan J 2016 Hydrodynamic interactions enhance gelation in dispersions of colloids with short-ranged attraction and long-ranged repulsion *Soft Matter* **12** 7670–81
- [249] Allen R J, Valeriani C and ten Wolde P R 2009 Forward flux sampling for rare event simulations *J. Phys.: Condens. Matter* **21** 463102
- [250] Charbonneau P, Kurchan J, Parisi G, Urbani P and Zamponi F 2014 Fractal free energy landscapes in structural glasses *Nat. Commun.* **5** 3725
- [251] Klongvessa N, Ginot F, Ybert C, Cottin-Bizonne C and Leocmach M 2019 Active glass: ergodicity breaking dramatically affects response to self-propulsion *Phys. Rev. Lett.* **123** 248004